Escalating Heatwave Activity and Return Periods Across the Climatic Zones of Ghana

Edmund I. Yamba[1*], Daniel Amponsah[1,2], Nana Ofosuhene Pinkrah[1,3], Stephen Oppong[1,4], Cosmos S. Wemegah[5], Mary J. Adjei[1], Alex K. Ablerdu[1]

1 Department of Meteorology and Climate Science, Kwame Nkrumah University of Science and Technology, Kumasi, Ghana

2 Department of Biosystems and Agricultural Engineering, Oklahoma State University, USA

3 Department of Earth, Environmental and Atmospheric Sciences, Western Kentucky University, USA

4 Department of Atmospheric Sciences, University of Utah, USA

5 Department of Atmospheric and Climate Science, University of Energy and Natural Resources, Sunyani, Ghana

* eiyamba@knust.edu.gh

Abstract

Heatwaves are an increasing public health concern in West Africa, yet their characteristics and recurrence across Ghana's climatic zones remain poorly quantified. Previous assessments in Ghana have largely focused on individual cities and percentile-based thresholds, which characterize extremes relative to the local climatology but do not explicitly account for recently experienced thermal conditions. Here, we assess the characteristics and return periods of heatwaves across Ghana's climatic zones using the Excess Heat Factor (EHF) framework. We analyzed quality-controlled daily maximum and minimum temperatures from 24 Ghana Meteorological Agency synoptic stations spanning 1960–2022. Heatwaves were defined as at least three consecutive days with EHF > 0 and characterized in terms of occurrence, frequency, duration, and intensity. Return levels of heatwave intensity and duration were estimated for 2–50-year return periods using Peaks-Over-Threshold modelling with the Generalized Pareto distribution. All climatic zones exhibited significant warming, transitioning from predominantly cooler conditions in the 1960s–1970s to sustained warming from the mid-1980s, with minimum temperatures increasing more rapidly than maximum temperatures in most zones and reducing nocturnal thermal relief. Heatwave activity increased markedly thereafter, with total heatwave days increasing significantly across all zones ($p < 0.001$) and fastest in the Coastal (0.70 days year^{-1}) and Forest (0.54 days year^{-1}) zones. Heatwave episodes were concentrated mainly between February and April. Heatwave intensity generally increased northward, whereas duration increased southward, and this contrast became more pronounced toward longer return periods. At the 50-year return period, the Sudan Savannah exhibited a high-intensity but comparatively short heatwave return level (≈12.5 °C^2; ≈21 days), whereas the Coastal zone exhibited substantially lower intensity but greater persistence (≈3.5 °C^2; ≈39 days), although uncertainty increased at longer return periods. These findings demonstrate that heatwave hazard in Ghana is intensifying but spatially differentiated, with rare events characterized predominantly by intensity in the north and persistence in the south. The results provide a quantitative climatological basis for developing climate-zone-specific heatwave monitoring and, with appropriate impact-based validation, a national heat-health early-warning framework for Ghana.

Keywords: Excess Heat Factor; heatwaves; climatic zones; Return Levels; Ghana; Generalized Pareto Distribution.

Author summary

Heatwaves are an increasing concern in West Africa, but how they are changing across Ghana's different climatic zones remains poorly understood. We examined heatwave activity across Ghana using daily temperature observations from 24 meteorological stations covering 1960–2022. We used the Excess Heat Factor, which identifies unusually hot conditions relative to both the long-term local climate and temperatures experienced during the preceding period. We found substantial warming across all climatic zones, particularly since the mid-1980s, with nighttime temperatures increasing faster than daytime temperatures in most zones. Heatwave activity has also increased significantly, with episodes occurring mainly between February and April. Importantly, heatwave hazard differs across Ghana: northern zones experience more intense heatwaves, whereas southern zones experience longer-lasting events and faster increases in total heatwave days. These differences become more pronounced for rare events. At a 50-year return period, heatwave intensity and duration are approximately 12.5 $^{\circ}C^2$ and 21 days in the Sudan Savannah, compared with approximately 3.5 $^{\circ}C^2$ and 39 days in the Coastal zone, although uncertainty increases for such rare events. These findings show that heatwaves are intensifying differently across Ghana and support climate-zone-specific approaches to heatwave monitoring and preparedness.

1 Introduction

Heatwaves are prolonged periods of unusually high temperatures relative to the prevailing climatological conditions of a location [1, 2]. As the climate warms, the frequency, duration and intensity of heatwaves are increasing in many areas, with important consequences for human health, agriculture, energy systems, and ecosystems [3]. Prolonged exposure to extreme heat is associated with increased heat-related morbidity and mortality, particularly among vulnerable populations such as older adults, pregnant women, and people with pre-existing health conditions [4–7]. Extreme heat is also associated with reduced crop productivity and increased livestock losses [8], while elevated cooling demand during hot periods has placed high pressure on electricity systems [9, 10]. These impacts are amplified by changes in land-use, land degradation, deforestation, and urbanization, including the effect of heat-islands in densely built environments [11, 12].

In recent decades, heatwave activities have increased in many parts of Africa [3, 13–16], with climate projections suggesting the worst scenario [17, 18]. In West Africa, complex interlocking factors such as high background temperatures, rapid population growth, climate-sensitive livelihoods, expanding urban areas, and limited adaptive capacity make the case of the region more concerning. For example, the exceptional heatwave experienced in parts of the Sahel and West Africa in early 2024 was associated with severe societal and health consequences [19]. Despite this high vulnerability level of the area, the detection and characterization of heatwaves remains comparatively limited, restricting our understanding of how rapidly the hazard is evolving and how it varies among climatic regimes. Ghana provides an important example setting for examining such variability. Although relatively small geographically, the country has a pronounced climatic gradient from humid coastal and forest environments in the south to considerably drier savannah environments in the north [20]. It exhibits differences in rainfall regimes, vegetation, atmospheric moisture, seasonality, and background temperature, which can influence both the occurrence and persistence of heatwaves. Therefore, understanding the characteristics of heatwaves in different climate environments is important for assessing heat-risk, planning adaptation, and the development of effective early-warning systems.

In Ghana, Wemegah et al. [21] examined the characteristics and trends of heatwaves in Accra, Kumasi, and Tamale, providing evidence of changing daytime and nighttime heatwave conditions in three major cities. Adjei et al. [22] assessed thermal stress and heat-related health risks using the Universal Thermal Climate Index (UTCI) and Humidex as bioclimatic indices, while Klutse et al. [23] examined historical and projected temperature changes in northern Ghana. Collectively, these studies demonstrate the growing significance of extreme heat in Ghana and provide an important basis for understanding heat-related hazards in the country. In particular, the work of Wemegah et al. [21] represents an important step towards characterizing heatwaves in Ghana and provides a basis for the development of heatwave monitoring and early-warning systems. However, although percentile-based methods are widely used to characterize heatwaves [24], their reliance on climatological thresholds alone does not adequately account for short-term physiological acclimatization or the compound effects of daytime and nighttime heat [25, 26]. Consequently, exceedance of a climatological percentile does not necessarily distinguish between temperatures that are extreme relative to the long-term climate and conditions that are also unusually hot relative to those experienced during the immediately preceding period. This distinction is particularly relevant in persistently warm environments such as Ghana, where recent thermal exposure can influence the significance of an extreme-heat episode [27–29]. These methodological and geographical limitations leave several important aspects of heatwave risk in Ghana unresolved. It remains unclear whether a framework that

incorporates both climatological extremes and recent thermal acclimatization reveals systematic differences in heatwave activity across Ghana's contrasting climatic zones. Moreover, the spatial variability of heatwave intensity and duration, their long-term evolution across the country, and the magnitude and persistence of rare heatwave events associated with different return periods have not been comprehensively quantified across these zones. Addressing these gaps is essential for developing a nationally coherent, yet climate-zone-specific, understanding of heatwave hazards and for providing an evidence base for heat-health early-warning and preparedness in Ghana.
The Excess Heat Factor (EHF) framework provides an approach for integrating these dimensions of extreme heat [25]. It combines a measure of climatological significance, which determines whether a short period of elevated mean temperature is unusually hot relative to the long-term local climate, with an acclimatization component that evaluates recent heat relative to temperatures experienced during the preceding period [25, 30, 31]. EHF is calculated from daily mean temperature derived from both maximum and minimum temperatures, thereby allowing both daytime and nighttime temperature conditions to contribute to the characterization of a heatwave rather than relying on daytime maximum temperature alone [25, 30]. This feature is particularly relevant for Ghana, where elevated nighttime temperatures can reduce nocturnal thermal relief and contribute to sustained heat exposure. Applying EHF across Ghana's climatic zones therefore provides a complementary framework for evaluating heatwaves in relation to both the long-term local climate and recently experienced thermal conditions.

In this study, we assessed the characteristics and return periods of heatwaves across Ghana's climatic zones using the EHF framework. Specifically, we addressed three questions: (1) How has heatwave activity, in terms of occurrence, frequency, duration, and intensity, evolved across Ghana over the 1960–2022 period? (2) How does the spatial distribution and seasonal timing of heatwave activity vary among Ghana's climatic zones? and (3) How do the return levels of heatwave intensity and duration vary among the climatic zones with increasing return periods? By addressing these questions, this study extends existing city-level evidence to a climatic-zone-scale assessment of heatwave hazard across Ghana and provides a quantitative basis for geographically differentiated heat-risk monitoring, adaptation planning, and the development of a national heatwave early-warning framework.

2 Materials and Methods

2.1 Study area

The study focused on the climatic zones of Ghana, namely the Sudan, Guinea, Transition, Forest and coastal zones (see Fig 1). These zones experience a tropical monsoon climate governed by the West African Monsoon (WAM) [32, 33] with each zone having a distinct climate characteristic [20]. The Sudan Savannah has the longest and harshest dry season, spanning the period November to May, with a maximum temperature of up to 40°C, especially in March and April. Rainfall is uni-modal with seasonal rain occurring between June and October and an annual total ranging from 600 to 1000 mm [34]. The Guinea Savannah zone has a mixture of grasslands and sporadic trees [35]. Rainfall in this zone is also uni-modal, with seasonal rainfall between May and October and an annual average total ranging between 1000 and 1200 mm. The dry season spans from November to April with a maximum temperature of up to 38°C [20]. For both zones, the humidity is generally low compared to the south, but generally higher in the Guinea Savannah compared to the Sudan Savanna. The southern part of Ghana, which comprises the transition, forest and coastal zones, has a cooler temperature compared to the north and a bimodal rainfall distribution. The first rainy season runs from March to July, with a peak in June, while the second season runs from September to mid-November, with a peak in October. Between December and February, the harmattan, which is a north-easterly desert wind, dominates the entire country. The Harmattan winds, which bring dry and dusty conditions from the Sahara Desert during the peak of the dry season, have an additional impact on this climatic pattern [36]. The harmattan wind is more prevalent in the north, lowering the humidity of the country during this period and also resulting in hotter days and cooler nights [33].

2.2 Data

Daily minimum (Tmin) and maximum (Tmax) temperature data from 24 synoptic stations (distributed across the country (see Fig 1)) spanning 1960 to 2022 were obtained from the Ghana Meteorological Agency (GMet). The raw data from each station were subjected to a series of quality control (QC) procedures to ensure accuracy, consistency, and suitability as follows:

i. **Missing dates**: We verified that complete daily records existed for each location for the entire study period by matching calendar days (1960-2022) to the dataset. Missing dates were inserted and their respective temperature records assigned a placeholder value of -99.

ii. **Outliers**: Ghana's Tmin and Tmax typically fall between 18-40^o [20]. Hence, we checked the data to ensure that the temperature data fell within a physical plausible range of 12°C to 50°C. Dates with records outside this range were considered outliers and replaced by a placeholder value of -99.

iii. **Non-numeric values**: We checked for possible temperature entries that cannot be interpreted as valid numbers. Any such non-numeric values were replaced by -99.

iv. **Internal consistency**: Days where Tmin $\geq$ Tmax were flagged as invalid and hence replaced by -99

v. **Repeated daily values**: Daily records repeated for 5 or more consecutive days were considered unusual. These dates were also flagged and replaced by a placeholder of -99.

The percentage of daily data available for each location after QC is shown in Table 1. Stations (bolded) with $\geq$ 80% of both Tmin and Tmax data were used in the analysis. Fig SM1-SM5 in the supplementary material (SM) shows the dates flagged with -99 after the QC process. To ensure that the stations used in the analysis had complete timeseries, we filled the missing values (-99) using daily 2m minimum and maximum temperature data from the European Center for Medium-Range Weather Forecasts (ECMWF) ERA5 reanalysis product [37]. ERA5 offers high spatial (0.25° × 0.25°) and

Table 1. Percentage of daily Tmax and Tmin data available after QC. Stations (bolded) with ≥ 80% of both Tmin and Tmax data were used in the analysis.

Station	Longitude	Latitude	Available Tmax [%]	Available Tmin [%]
Navrongo	-1.10	10.90	97.24	91.28
Zuarungu	-0.81	10.80	97.32	91.28
Wa	-2.50	10.05	95.50	95.83
Bole	-2.48	9.03	95.15	98.23
Tamale	-0.85	9.43	97.09	93.44
Yendi	-0.02	9.45	96.28	94.82
Kete Krachi	-0.17	7.80	95.97	98.64
Sunyani	-2.30	7.33	92.35	99.62
Wenchi	-2.10	7.74	90.16	98.31
Ho	0.48	6.61	89.06	99.96
Koforidua	-0.25	6.08	76.41	99.81
Kumasi	-1.62	6.68	89.48	99.95
Abetifi	-0.75	6.67	92.20	99.83
Sefwi Bekwai	-2.32	6.20	89.71	99.86
Akuse	0.12	6.10	87.03	99.96
Akim Oda	-0.97	5.93	88.44	99.91
Accra	-0.17	5.65	81.08	100.00
Ada	0.61	5.79	36.68	81.08
Akatsi	0.80	6.12	81.76	98.67
Axim	-2.24	4.87	42.90	92.80
Saltpond	-1.05	5.20	56.87	99.66
Takoradi	-1.77	4.88	54.10	99.96
Tema	0.02	5.70	85.44	99.63

temporal resolution and has been validated for meteorological research in Africa [38–40]. ERA5 data were extracted for each location using their geographical coordinates (see Table 1) and used to fill the corresponding days in the observed GMet data with -99 placeholder values. Using the completed daily Tmin and Tmax timeseries, the daily mean/average temperature (Tmean) was also calculated for each location by averaging the corresponding daily Tmin and Tmax values.

2.3 Analysis

2.3.1 Trends in annual Tmin, Tmean and Tmax anomaly

For each station in each climatic zone, we computed the Standardized Temperature Anomaly Index (STAI) for Tmin, Tmean and Tmax at the annual time scale using equation 1:

$$\text{STAI}_n = \frac{X_n - \mu}{\sigma} \tag{1}$$

where X_n is the annual temperature for year n, μ is the long-term climatological mean over the full study period, and σ is the corresponding standard deviation. The magnitude of STAI reflects the degree of departure from the mean, indicating warming or cooling. Positive STAI values indicate warmer than average years while negative values indicate cooler-than-average years. STAI has been widely applied to characterize the signals of warming and drought in tropical climates [20, 41]. Moreover, the rate and significance of the warming signal in the Tmin, Tmean and Tmax series were assessed using the non-parametric Mann–Kendall test together with the Theil–Sen slope estimator, with the magnitude of the trend expressed in °C per decade and the significance evaluated at the confidence level of 95%. The Mann–Kendall test is robust to non-normality and outliers, while the Theil–Sen estimator provides a robust estimate of the trend magnitude that is insensitive to extreme values [42].

2.3.2 Identifying and characterizing heatwaves

Heatwaves were identified using the EHF method. The EHF is an index that combines two complementary measures of excess heat, in which one captures how extreme a period is relative to long-term climate, and the other captures how anomalous it is relative to recent conditions to which the population has adapted [25]. This dual-index structure makes the EHF particularly suitable for Ghana, where populations are generally acclimatized to high baseline temperatures, but remain physiologically vulnerable to sustained anomalous heat. The EHF has been shown to outperform percentile-based metrics as a predictor of heat-related mortality and morbidity, and is now applied operationally in several national heat-warning systems [26, 30, 43, 44]. The following computational procedure for EHF, as described by Narin et. al. [25], was followed to detect heat waves:

Step 1: Computing Daily Mean Temperature. The daily mean temperature for day i, denoted T_i, was calculated as the arithmetic mean of daily Tmax ($T_{\max,i}$) and daily Tmin ($T_{\min,i}$) as shown in eqn 2:

$$T_i = \frac{T_{\max,i} + T_{\min,i}}{2}. \quad (2)$$

This formulation incorporates both daytime and nighttime temperatures, thereby reflecting cumulative thermal stress more fully than the daily maximum temperature alone, as used in the percentile threshold method.

Step 2: Climatological Threshold. A climatological threshold temperature, T_{95}, was defined as the 95th percentile of the daily mean temperature ($\mathrm{T_i}$) of each station at each zone over the full study period (1960–2022). This percentile was calculated using all calendar days of the year pooled together (i.e., without separating by day-of-year), consistent with the original EHF formulation [25]. This threshold represents the temperature above which conditions are considered climatologically extreme for that station.

Step 3: Three-Day Period Mean Temperature. Because heat stress accumulates over several consecutive days rather than isolated days, the EHF is based on three-day periods (TDPs). The mean temperature of the TDP ending on day i was calculated as the average of day i and the two preceding days using eqn 3 below:

$$\bar{T}_i^{(3)} = \frac{T_i + T_{i-1} + T_{i-2}}{3}. \tag{3}$$

Step 4: Excess Heat Indices: Two complementary EHI, namely significance and acclimatization, were computed from the TDP mean. The *significance index* ($\mathrm{EHI_{sig}}$), measures how hot the TDP is relative to the long-term climate by comparing it to the climatological threshold. This was done using eqn 4 below:

$$\mathrm{EHI_{sig}}(i) = \bar{T}_i^{(3)} - T_{95}. \tag{4}$$

A positive $\mathrm{EHI_{sig}}$ indicates that the mean temperature of three-days exceeds the 95th percentile of the long-term record, signifying a climatologically rare warm period. The *acclimatization index* ($\mathrm{EHI_{accl}}$), measures how hot the TDP is relative to the temperatures experienced during the 30 days immediately preceding it, the period over which the body physiologically adapts to ambient heat. This was done using eqn 5 below:

$$\mathrm{EHI_{accl}}(i) = \bar{T}_i^{(3)} - \frac{1}{30}\sum_{k=3}^{32} T_{i-k}. \tag{5}$$

The averaging window in eqn 5 spans days $i-3$ to $i-32$ and therefore does not overlap the three-day period in eqn 3. A positive $\mathrm{EHI}_{\mathrm{accl}}$ indicates that the current TDP is hotter than the recent thermal background, meaning that even populations acclimatized to high baseline temperatures face an additional heat burden. Together, the two indices capture situations where temperatures are both historically extreme and anomalously high relative to what a population has recently experienced.

Step 5: Excess Heat Factor. The EHF is defined as the product of $\mathrm{EHI}_{\mathrm{sig}}$ and $\max(1, \mathrm{EHI}_{\mathrm{accl}})$ (eqn 6):

$$\mathrm{EHF}(i) = \mathrm{EHI}_{\mathrm{sig}}(i) \times \max\big(1,\, \mathrm{EHI}_{\mathrm{accl}}(i)\big). \tag{6}$$

The $\max(1, \mathrm{EHI}_{\mathrm{accl}})$ term ensures that when acclimatization conditions are not anomalous (i.e., $\mathrm{EHI}_{\mathrm{accl}} \leq 1$), the EHF still reflects the significance component without being diminished below it. The multiplicative structure preserves the sign of $\mathrm{EHI}_{\mathrm{sig}}$: the EHF is positive only when the TDP is climatologically extreme (i.e., $\mathrm{EHI}_{\mathrm{sig}} > 0$), and its magnitude is amplified when the acclimatization anomaly is also positive. The resulting EHF has units of $^{\circ}\mathrm{C}^2$ [45].

Step 6: Heatwave Metrics. The following heat wave metrics were determined:

- **Heatwave day**: a calendar day with $\mathrm{EHF}(i) > 0$. Conversely, a non-heatwave day is a day with $\mathrm{EHF}(i) \leq 0$.
- **Heatwave event (episode)**: three or more consecutive heatwave days, i.e. a run of three or more days with $\mathrm{EHF}(i) > 0$.
- **Prevalence**: the number or fraction of years within the study period that recorded at least one heatwave episode, providing a broad measure of how widespread and recurring heatwave conditions have been over time.
- **Frequency**: the number of distinct heatwave episodes per year.
- **Duration**: the length of a heatwave episode, measured as the number of consecutive heatwave days, ranging from the minimum of three days to multi-week events. The mean and maximum duration of the episode were calculated per zone.

- **Intensity**: a measure of the thermal severity of an episode. The mean intensity of an episode comprising n heatwave days is given by eqn 7:

$$I_{\text{mean}} = \frac{1}{n}\sum_{j=1}^{n} \text{EHF}(j), \tag{7}$$

  where the summation runs over the positive-EHF days that constitute the episode. The peak intensity of an episode, $I_{\text{peak}} = \max_j \text{EHF}(j)$, was also recorded. The intensity of the peak per-episode I_{peak} and the duration of the episode were retained as exceedance variables for the extreme value analysis described below.

The long-term trends in total annual heatwave days (the sum of all heatwave days in a given year) were assessed using ordinary least squares regression, and the estimated rate of change (days per year) was reported along with its statistical significance. A five-year rolling mean was also computed to smooth interannual variability and highlight decadal-scale shifts.

2.3.3 Heatwave return period

We quantified the probability and expected magnitude of rare but severe heatwave events by applying the Peaks-Over-Threshold (POT) approach. The POT was preferred because it models exceedances of a high threshold rather than only block maxima, and therefore makes fuller use of the record and avoids the years with no events that would otherwise enter a block-maxima series as structural zeros [46]. Under the POT framework, the exceedances of an independent variable above a sufficiently high threshold u asymptotically follow the Generalised Pareto Distribution (GPD) [46, 47]. For an excess $y = x - u \geq 0$, the GPD cumulative distribution function is:

$$G(y;\sigma,\xi) = \begin{cases} 1 - \left(1 + \dfrac{\xi y}{\sigma}\right)^{-1/\xi}, & \xi \neq 0, \\ 1 - \exp\left(-\dfrac{y}{\sigma}\right), & \xi = 0, \end{cases} \tag{8}$$

defined for $y \geq 0$ and $1 + \xi y/\sigma > 0$, where $\sigma > 0$ is the **scale parameter** and ξ is the **shape parameter** governing the tail: $\xi < 0$ gives a bounded upper tail, $\xi = 0$ the exponential limit, and $\xi > 0$ a heavy, unbounded tail.

The Extreme Value Analysis (EVA) was performed separately on two exceedance variables in each zone: the per-episode peak intensity I_{peak} (in $^{\circ}\text{C}^2$) and the episode duration (in days). Because the EHF construction already isolates climatologically extreme periods, the set of detected heatwave episodes constitutes the peaks over threshold, and each episode contributes a single, declustered exceedance. The threshold u was therefore taken at the EHF heatwave criterion for intensity and at the minimum episode length for duration; the adequacy of these thresholds was confirmed using mean-residual-life and parameter-stability diagnostics [48, 49].

The GPD parameters (σ, ξ) were estimated for each zone and variable by Maximum Likelihood Estimation (MLE), with the shape parameter constrained to the range $-0.5 \leq \xi \leq 0.5$ to ensure numerically stable fits given the sample sizes. Goodness-of-fit was evaluated using the Kolmogorov–Smirnov (K–S) test and return-level plots, confirming that the GPD provided an adequate fit to the empirical exceedances in all zones. The return level z_T, defined as the value expected to be exceeded on average once every T years, is obtained from the fitted GPD as shown in eqn 9 [47]:

$$z_T = \begin{cases} u + \dfrac{\sigma}{\xi}\left[(\lambda T)^{\xi} - 1\right], & \xi \neq 0, \\ \\ u + \sigma \ln(\lambda T), & \xi = 0, \end{cases} \tag{9}$$

which is defined for $\lambda T > 1$. Return levels were estimated for recurrence intervals of $T = 2, 5, 10, 20,$ and 50 years for both EHF peak intensity and heatwave duration in each climatic zone. The 95% confidence intervals on the return levels were obtained by parametric bootstrap (1,000 resamples), which is preferred over the nonparametric bootstrap for the small samples typical of extreme-value models [50] and which propagates the uncertainty in the fitted GPD parameters through eqn 9. These return levels quantify the magnitude of heatwave events that infrastructure, public health systems, and agriculture may need to withstand at different probabilities of occurrence, providing actionable benchmarks for climate risk assessment and adaptation planning [51–53].

Table 2. Trends in annual Tmax, Tmin, and Tmean temperature for each stations used in the study. The values shows the magnitudes of the trends (Sen's slope (°C per decade)) and their significance level (p-value) in parentheses. Stations with $^{*}p < 0.05$ are significant, $^{**}p < 0.01$ are highly significant, $^{***}p < 0.001$ are extremely significant and those with ($p > 0.05$) are not significant.

Zone	Station	T_{max}	T_{min}	T_{mean}
Sudan Savannah	Navrongo	0.146 (0.001)***	0.265 (<0.001)***	0.189 (<0.001)***
	Zuarungu	0.123 (0.265)	0.390 (<0.001)***	0.200 (<0.001)***
Guinea Savannah	Wa	0.226 (<0.001)***	0.317 (<0.001)***	0.243 (<0.001)***
	Bole	0.170 (0.001)***	0.399 (<0.001)***	0.260 (<0.001)***
	Tamale	0.128 (0.013)*	0.309 (<0.001)***	0.208 (<0.001)***
	Yendi	0.203 (<0.001)***	0.374 (<0.001)***	0.295 (<0.001)***
	Kete Krachi	0.201 (<0.001)***	0.270 (<0.001)***	0.212 (<0.001)***
Transition	Sunyani	0.266 (<0.001)***	0.210 (<0.001)***	0.236 (<0.001)***
	Wenchi	0.154 (<0.001)***	0.294 (<0.001)***	0.218 (<0.001)***
Forest	Ho	0.163 (0.001)***	0.283 (<0.001)***	0.198 (<0.001)***
	Kumasi	0.328 (<0.001)***	0.311 (<0.001)***	0.302 (<0.001)***
	Akim Oda	0.444 (<0.001)***	0.280 (<0.001)***	0.341 (<0.001)***
	Sefwi Bekwai	0.396 (<0.001)***	0.317 (<0.001)***	0.340 (<0.001)***
Coastal	Accra	0.150 (<0.001)***	0.366 (<0.001)***	0.250 (<0.001)***
	Akatsi	0.406 (<0.001)***	0.122 (<0.001)***	0.347 (<0.001)***
	Tema	0.300 (<0.001)***	0.364 (<0.001)***	0.337 (<0.001)***

3 Results

3.1 Trends in annual Tmax, Tmin, and Tmean anomalies.

Table 2 shows the results of the Mann-Kendall trend analysis performed on annual Tmax, Tmin, and Tmean for each station. In general, all stations indicate the existence of upward temperature trends with almost all stations showing highly significant ($p < 0.001$) trends except for Zuarungu, which showed an insignificant ($p > 0.05$) Tmax trend. All stations at Sudan and Guinea Savannah zones demonstrated stonger trends in Tmin compared to Tmax. In the Transition zone, Wenchi showed a stronger Tmin trend than its Tmax, while Sunyani showed higher magnitude in Tmax than its Tmin. In the Forest zone, all stations except Ho, showed higher Tmax trends than Tmin. In the Coastal zone, both Accra and Tema demonstrate higher Tmin trends than Tmax while Akatsi showed the opposite. In a nutshell, annual trends in Tmax, Tmin, and Tmean were higly significant over the study period.

Similarly, Fig 2 presents the trends in standardized anomalies of annual Tmax, Tmin, and Tmean for the five climatic zones of Ghana over the study period (1960–2022). Across all zones, the early decades (1960s to late 1970s) are characterized by predominantly negative temperature anomalies. The most pronounced cooling are evident in the Sudan Savannah, where Tmin anomalies dropped to nearly -3.5°C around

1968, and in the Guinea Savannah, which recorded a Tmax anomaly of approximately -4.0°C around 2014. From the mid-1980s onward, a clear and sustained shift toward positive anomalies is observed across all zones, with the post-2000 period dominated by persistent above-average temperatures. Warming rates differ across zones and temperature metrics. Tmin warmed faster than Tmax in four of the five zones, the exception being the Transition zone, where Tmax warmed at 0.266°C/decade compared to Tmin at 0.210°C/decade. The strongest Tmin warming was recorded in the Coastal zone at 0.366°C/decade, followed by the Forest zone (0.311°C/decade) and Guinea Savannah (0.309°C/decade). For Tmax, the Forest zone recorded the highest rate at 0.328°C/decade, while the Guinea Savannah recorded the lowest at 0.128°C/decade. Tmean warming rates ranged from 0.189°C/decade in the Sudan Savannah to 0.302°C/decade in the Forest zone.

3.2 Heatwave prevalence, duration and intensity

Fig 3 – 7 present the temporal distribution, frequency, duration, and mean intensity of heatwave episodes for the individual stations in each climatic zone. In every panel, each bar is positioned on its day-of-year of onset, its height equals the duration of the episode, and its color denotes the mean intensity of EHF; the number above each bar is the duration of the episode in days.

In the northern savannah zones (see Fig 3 and 4, isolated episodes first appeared in the mid-1960s, with only sporadic activity through the 1970s. The frequency of episodes is observed to then increase steadily from the 1980s and accelerate after 2010, producing dense clustering in the later years of the research period. Episodes are strongly concentrated between day-of-year 30 and 150 (February–May), peaking in February–April, with few events outside this window. Most episodes last between 3 and 6 days (mean ≈ 6.1 days in the Sudan Savannah and ≈ 7.1 days in the Guinea Savannah), but individual episodes can be far longer. The longest episode reached 26 days in the Sudan Savannah (in 2005) and 41 days in the Guinea Savannah (in 2019 occurring as the longest single episode recorded in all zones). The most intense episodes (deep red) occurred in the Guinea Savannah, including a short high-intensity event near the start of 1998. The highest single-day EHF value was approximately 5.0°C^2 in the

Guinea Savannah and 4.5°C^2 in the Sudan Savannah.

The transition zone (Fig 5) recorded the earliest activity, with isolated episodes in the early 1960s followed by a sparse occurrence through the 1970s, while the forests (Fig 6) and Coastal (Fig 7) zones showed virtually no episodes before the early 1980s. From the mid-1980s onward, all three zones displayed rising episodes, with a marked increase and dense clustering towards the end of the research period. The total episode counts were 99 for the Transition, 92 for the Forest, and 114 for the Coastal zone. Most episodes lasted between 3 and 6 days (mean ≈ 7.4, 7.5, and 6.8 days in the Transition, Forest, and Coastal zones, respectively). These southern zones produced some of the longest individual episodes of the study, reaching 35 days in the Transition zone (1998) and 34 days in the Coastal zone (1998), with the Forest zone reaching 29 days (2016). The mean intensities of episodes are generally lower than in the northern zones, ranging from about 0.25 to 1.8°C^2, with the Transition zone recording the highest values among the three zones. The most intense episodes in all three zones are concentrated in the post-2015 period. Seasonally, episodes in the Transition and Forest zones are concentrated between day-of-year 30 and 150 (February–May), while the Coastal zone showed by far the widest seasonal spread, with episodes distributed throughout the year, including late-year events near day-of-year 290–360, particularly after 2015.

3.3 Total Heatwave days and trends

Fig 8 shows the total annual heat wave days for each zone, the rolling mean of 5-years (dark red line), and the fitted linear rate of change. All five zones showed a pronounced interannual variability superimposed on a statistically significant upward trend ($p < 0.001$ in every zone). The Sudan Savannah increases at 0.29 days per year; despite large fluctuations from year-to-year, its rolling mean rises from near zero in the 1960s–1970s to roughly 15–25 days in the most recent decades. The Guinea Savannah increases at 0.45 days per year, with totals increasing dramatically after the late 1990s and the rolling mean reaching its highest values (≈35–40 days) after 2015. The Transition zone increases at 0.35 days per year, with relatively low totals before the 1980s and a clear rise from the 2010s. The forests and Coastal zones showed the steepest trends, at 0.54 and 0.70 days per year, respectively. In both, totals were near zero before the early

Table 3. Station-level trends in annual total heatwave days for each climatic zone. Values are the ordinary-least-squares rate of change (days per year) with the p-value in parentheses. Levels of significance include: $^{*}p < 0.05$ are significant, $^{**}p < 0.01$ are highly significant, $^{***}p < 0.001$ extremely significant.

Zone	Station	Trend (days/year)
Sudan Savannah	Navrongo	0.29 (<0.001)***
	Zuarungu	0.41 (<0.001)***
Guinea Savannah	Wa	0.41 (<0.001)***
	Bole	0.46 (<0.001)***
	Tamale	0.45 (<0.001)***
	Yendi	0.68 (<0.001)***
	Kete Krachi	0.28 (<0.001)***
Transition	Sunyani	0.35 (<0.001)***
	Wenchi	0.38 (<0.001)***
Forest	Ho	0.27 (0.014)*
	Kumasi	0.54 (<0.001)***
	Akim Oda	0.44 (<0.001)***
	Sefwi Bekwai	0.44 (<0.001)***
Coastal	Accra	0.70 (<0.001)***
	Akatsi	0.46 (<0.001)***
	Tema	0.84 (<0.001)***

1980s and rose steeply after 2015, with the Coastal zone reaching the highest annual totals of any zone, approaching 90 days in the most recent years.

Table 3 reports the station-level trends in annual total heatwave days. All stations showed extremely significant positive trends, but Ho. These station rates bracket the corresponding zonal rates (shown in Fig. 8) supporting the zonal trends revealed therein. The fastest station-level rates occurred in Tema (0.84 days per year) and Accra (0.70) in the Coastal zone, alongside Yendi (0.68) in the Guinea Savannah. The rates at the Sudan Savannah stations were slower compared to other zones (for example, Navrongo at a rate of 0.29 days per year).

3.4 Return Levels of Heatwave Intensity

Fig 9 shows the peak-over-threshold (POT) return levels of EHF intensity (left panel) and heatwave duration (right panel) for return periods of 2, 5, 10, 20 and 50 years in the five climatic zones, with shaded 95% confidence bands. Spatially, the EHF intensities are observed to be high in the northern zones and low in the southern zones (i.e show a southward decrease); whiles the durations are longest in the southern zones and shortest in the northern zones (i.e duration show a northward decrease). For example, intensities in the Guinea and Sudan Savannah zones increased roughly from around 3.0°C^2 during the 2-year return period to a maximum of approximately 15 °C^2 during the 50-year return period. The intensities in the Transition and Forest zone are maximum around around 10.0°C^2) while the Coastal zone consistently records the lowest intensities (maximum intensities lower than 6.0°C^2). However, the duration followed the reverse gradient. All zones cluster near 7 days in the 2-year return period, but the curves diverge at longer return periods. The Coastal zone showed the longest duration throughout (approximately 39 days in the 50-year return period), followed by the forests (≈34), transition (≈33), the Guinea Savannah (≈30) zones and the Sudan Savannah with the shortest duration (≈ 21 days). Consequently, in the 50-year return period, the Sudan Savannah combines the joint-highest intensity (≈12.5°C^2) with the shortest duration (≈21 days), while the Coastal zone combines the lowest intensity (≈3.5°C^2) with the longest duration (≈39 days); confidence bands widen with the return period and overlap most for duration in longer return periods.

4 Discussion

This study assessed heatwave activity across the five climatic zones of Ghana (see Fig 1) using the EHF and multi-decadal data from the GMet revealing three main findings. First, warming over 1960–2022 has been sustained across the country, with minimum temperatures increasing more rapidly than maximum temperatures in most zones. Second, heatwave activity has increased markedly since the mid-1980s, with significant increases in heatwave days across all climatic zones and particularly rapid increases in the Coastal and Forest zones. Third, the intensity and persistence of the heatwaves exhibit contrasting spatial patterns. The northern Savannah zones experience the highest-intensity events, while the southern zones experience rare events of longer-duration and faster accumulation of heatwave days. Although uncertainty increases at longer return periods, fitted 50-year intensity return levels reach approximately 12.5 and 13.3 °C^2 in the Sudan and Guinea Savannah zones, respectively, compared to about 3.5 °C^2 in the Coastal zone. In contrast, the return level for 50-years is approximately 39 days in the Coastal zone compared to about 21 days in the Sudan Savannah. These results demonstrate that the escalation of heatwave hazard across Ghana cannot be described by a single north–south gradient. Rather, the intensity and persistence of extreme heat have different geographical expressions.

The transition from predominantly negative temperature anomalies before the late 1970s to persistent positive anomalies thereafter is consistent with the broader warming documented across tropical regions during recent decades [20, 21, 54]. An important feature of this warming is the stronger increase in minimum than maximum temperatures in four of the five climatic zones, with the Coastal zone recording a T_{min} trend of 0.366 °C per decade. Similar asymmetric warming has been documented at regional scales and has been associated with changes in atmospheric moisture and longwave radiation, as well as local influences such as land-use change and urban heat retention [12, 55, 56]. The strong increase in minimum temperature is important for heatwave characterization because warmer nights reduce the temperature decline that normally follows daytime heating [12, 57]. The daily-mean temperature formulation of EHF incorporates both maximum and minimum temperature conditions, while its acclimatization component additionally evaluates current heat relative to recently experienced temperatures [26]. It therefore provides information on sustained thermal anomalies that is not explicitly represented when heatwaves are defined solely by exceedance of a fixed maximum-temperature percentile.

The occurrence of heatwaves also exhibited a pronounced seasonal structure, with episodes mainly concentrated between February and April. This timing broadly corresponds to the late dry season and the transition to the West African monsoon, when high solar radiation, limited cloud cover and rainfall, and seasonally evolving continental and maritime influences can favor elevated surface temperatures [33, 58, 59]. The relative importance of these processes vary among Ghana's climatic zones, particularly because the seasonal evolution of rainfall, moisture and Harmattan influence differs substantially between northern and southern Ghana [20, 34]. Consequently, the February–April concentration identifies a common seasonal window within which the climatic conditions favorable for heatwave development occur across the different zones. The contrasting spatial behavior of the intensity and duration of the heatwaves is one of the most important findings of this study. The intensity of the heatwave generally increased northward, whereas the duration tends to increase southward, and this contrast becomes more pronounced for increasingly rare events. The high intensities observed in the northern zones (Sudan and Guinea Savannah zones) are consistent with the hot and semi-arid surface conditions of northern Ghana, where relatively sparse vegetation and seasonally low soil moisture can favor a greater partition of available surface energy into sensible heating [60, 61]. In contrast, the lower temperature variability associated with more humid southern zones (Forest and Coastal zones) can contribute to the persistence of warm anomalies once established [22, 62] , potentially favoring longer episodes even when their intensity of EHF is comparatively modest. This is because for areas such as the Forest and Coastal zones, high humidity can impose an additional physiological burden during periods of sustained high temperature [63, 64] even though relatively modest EHF intensities are observed in these areas. Interannual climate variability can modulate the timing and magnitude of individual heatwave episodes observed [65]. Some of the most intense events in the northern zones, including a short but intense episode near the beginning of 1998 in the Guinea Savannah and the clustering of episodes during the mid-2010s, occurred during periods that included major warm phases of the El Ni no–Southern Oscillation (ENSO). ENSO has previously been associated with variations in surface temperature in West Africa [66] and therefore interannual climate variability and ENSO could play a role in these intense events.

The direction of the observed changes is broadly consistent with previous studies across Africa and West Africa. Increases in heatwave frequency and intensity have been documented across the continent during recent decades [13, 67–69], while stronger nighttime warming has also been reported globally and regionally [21, 54, 70]. The February–April concentration identified here is consistent with previous evidence of elevated heatwave occurrence around the transition into the West African monsoon season [19, 71] and with the high-insolation conditions characteristic of the late dry season [58]. Similarly, the higher heatwave intensities observed in northern Ghana are consistent with evidence of increased extreme temperatures in semi-arid Savannah environments in West Africa [20, 72]. Within Ghana, the findings expand the city-level evidence provided by Wemegah et. al. [21], who examined heatwaves in Accra, Kumasi, and Tamale using percentile-based thresholds. The direction of change found here is

broadly consistent with that study for the climatic zones containing these cities, while the present analysis adds several dimensions. The rate at which heatwave days have accumulated in southern Ghana is particularly notable. The days of heatwaves increased by approximately 0.70 days per year in the Coastal zone and 0.54 days per year in the Forest zone, compared to approximately 0.29 days per year in the Sudan Savannah. These trends indicate an increasing contribution of sustained heatwave conditions to dry-season heat exposure in southern Ghana.
The return-period analysis further demonstrates that increasingly rare heatwaves have markedly different characteristics across Ghana's climatic zones. In the 2-year return period, the durations of the heat waves are relatively similar across the zones, clustering around 7 days. The fitted duration curves diverge progressively at longer return periods, reaching approximately 39 days in the Coastal zone, 34 days in the Forest zone, 33 days in the Transition zone, 30 days in the Guinea Savannah, and 21 days in the Sudan Savannah at the 50-year return period. The intensity of the heatwave showed the opposite spatial pattern, with the highest return levels in the northern Savannah zones and the lowest in the Coastal zone. Thus, rare heatwaves in northern Ghana are characterized primarily by high intensity, whereas those in southern Ghana are characterized more strongly by persistence. This distinction is potentially important for heatwave monitoring because intensity and duration represent different dimensions of hazard and may require different forms of preparedness.

The findings in this work have implications for heat-health monitoring, agriculture, and climate services, although the present study quantified the danger of heatwaves rather than the total risk of heat. From a public-health perspective, the combination of increased heat wave frequency and longer-duration events in southern Ghana can increase opportunities for prolonged heat exposure, while the higher absolute heatwave intensities in the northern zones indicate a different form of thermal hazard [5, 19]. These contrasting hazard profiles suggest that intensity and persistence should both be considered when developing heat-health monitoring systems. For agriculture, the concentration of heatwaves between February and April overlaps with an important seasonal transition in northern Ghana, where elevated temperatures and associated evaporative demand may intensify water stress in already moisture-limited environments

[8]. For climate services, the substantial inter-zonal differences in baseline temperature and heatwave behaviour argue against treating Ghana as thermally homogeneous. Daily-mean 95th-percentile thresholds range from approximately 29 °C in the Transition zone to nearly 34 °C in the Sudan Savannah, illustrating the different climatic baselines to which populations are exposed. A single absolute national temperature criterion could therefore represent substantially different levels of climatological extremity among zones. The relative and acclimatization-sensitive construction of EHF offers one framework for accounting for these local climatic differences [73–75]. Moreover, the consistent concentration of heatwave activity between February and April identifies a recurring period during which monitoring and preparedness could be strengthened, consistent with multi-sectoral heat early-warning approaches applied elsewhere [30].

This study has several strengths, including the use of a 62-year daily observational record spanning all five climatic zones of Ghana, the application of the EHF framework that integrates climatological excess with recently experienced thermal conditions, and the use of a peak-over-threshold approach to characterize rare heatwave events. Together, these features allowed long-term temporal changes, spatial and seasonal variability, and the behavior of rare heatwave events to be examined within a common analytical framework. Nevertheless, the following limitations are acknowledged especially when interpreting the findings. Firstly, EHF is calculated from Tmean, derived from Tmax and Tmin, and therefore does not explicitly account for atmospheric humidity. Our results consequently characterize the temperature-based heatwave hazard rather than the complete physiological heat stress. This distinction is particularly important in the humid southern zones, where atmospheric moisture may amplify the physiological effects of sustained high temperatures [63, 64]. In addition, the absence of co-located morbidity and mortality data precluded direct assessment of heat-related health impacts and the derivation or validation of health-protective warning thresholds. Therefore, our future work focuses on integrating temperature, humidity and health-outcome data in order to translate the climatological characteristics of heatwaves into impact-based heat-health warning criteria. Secondly, the physical mechanisms underlying the observed spatial contrast between heatwave intensity and duration were not explicitly evaluated. Processes involving surface-energy partitioning, soil moisture, vegetation state, and atmospheric moisture could provide physically plausible explanations for the contrasting heatwave characteristics of northern and southern Ghana, and these represent our future process-based analysis to unravel the relative contributions of these mechanisms to the observed intensity–duration contrast. Thirdly, the possible contribution of large-scale modes of interannual climate variability was not explicitly quantified. Although the timing of some prominent heatwave episodes coincided with major ENSO phases, ENSO indices were not statistically evaluated against heatwave occurrence, intensity, or duration. Future work would therefore examine the relationship between ENSO and heatwave variability explicitly and assess the extent to which interannual climate variability modulates the long-term warming signal.

5 Conclusion

Using the EHF across all five climatic zones of Ghana for 1960–2022, our study demonstrates that heatwave activity in the country is intensifying and that this intensification is neither spatially uniform nor seasonally diffuse. A sustained warming trajectory, characterized by disproportionately rapid increases in minimum temperatures, has reduced nocturnal thermal relief and coincided with increases in heatwave occurrence, frequency, duration, and intensity since the mid-1980s. Importantly, heatwave hazard is expressed differently across the country: the northern Savannah zones experienced the most intense events, whereas the southern Forest and Coastal zones are accumulating heatwave days fastest and exhibit the longest durations under rare-event conditions. This contrasting geography of intensity and persistence demonstrates that heatwave escalation in Ghana cannot be adequately characterized by a single national descriptor. The study also provides a zone-resolved baseline of heatwave behaviour across Ghana and extends previous city-scale assessments to all major climatic regimes of the country. The EHF framework complements percentile-based approaches by taking into account both climatological extremity and recent thermal conditions while incorporating maximum and minimum temperatures through daily mean temperature. The Peaks-Over-Threshold analysis further showed that the spatial contrast between intensity and duration becomes increasingly pronounced toward longer return periods. Rare heatwaves in northern Ghana are characterized primarily by high intensity, while those in southern Ghana are characterized more strongly by persistence. The substantial inter-zonal differences in heatwave characteristics, together with the recurrent concentration of episodes between February and April, support climate-zone-specific and seasonally targeted approaches to heatwave monitoring and preparedness. Translating these climatological findings into an operational heat-health early-warning system will require integration of humidity and health-outcome data, assessment of socioeconomic and infrastructural vulnerability, and validation of warning thresholds against observed impacts. Future work should also consider non-stationary extreme-value models and investigate the roles of interannual climate variability and other physical drivers of heatwave behavior.

Acknowledgments

The author thanks the Ghana Meteorological Agency for providing their data for this work.

Author Contribution

The work presented here was carried out collaboratively among the authors. Edmund I. Yamba: Conceptualization, Supervision, Data Curation, Methodology, and Writing-original draft. Daniel Amponsah: Formal Analysis, visualization, Software, Data Curation, Writing-original draft. Nana Ofosuhene Pinkrah: Formal Analysis, visualization, Software, Writing-review & editing. Stephen Oppong: Formal Analysis, visualization, Software, Writing-review & editing. Cosmos S. Wemegah: Conceptualization, Supervision, Writing-review & editing. Mary J. Adjei: Validation and Writing-review & editing. Alex K. Ablerdu: Validation and Writing-review & editing. All authors proofread the manuscript.

Financial Disclosure:

The authors received no funding for this work.

Competing Interest

The authors declare that they have no competing interests.

Code availability

All Data and codes used for STAI, Excess Heat Factor (EHF)/heatwaves computation, trend analysis, extreme value analysis (Peaks-Over-Threshold with the Generalized Pareto Distribution), and figure generation are available in a public GitHub repository: `https://github.com/climateandhealthresearchlab/Excess-Heat-Factor-Analysis`.

References

1. McCarthy M, Armstrong L, Armstrong N. A new heatwave definition for the UK. Weather (00431656). 2019;74(11).

2. World Meteorological Organization. International Meteorological Vocabulary. WMO-No. 182. Geneva, Switzerland: World Meteorological Organization; 2023. Accessed: July 3, 2025. Available from: `https://library.wmo.int/index.php?lvl=notice_display&id=22207`.

3. Masson-Delmotte V, Zhai P, Pirani A, Connors SL, Péan C, Berger S, et al. Climate change 2021: the physical science basis. Contribution of working group I to the sixth assessment report of the intergovernmental panel on climate change. 2021;2(1):2391.

4. Bell JE, Brown CL, Conlon K, Herring S, Kunkel KE, Lawrimore J, et al. Changes in extreme events and the potential impacts on human health. Journal of the Air & Waste Management Association. 2018;68(4):265-87.

5. Perkins-Kirkpatrick S, Lewis S. Increasing trends in regional heatwaves. Nature communications. 2020;11(1):3357.

6. Putsoane T, Bhanye JI, Matamanda A. Extreme weather events and health

inequalities: Exploring vulnerability and resilience in marginalized communities. Developments in Environmental Science. 2024;15:225-48.

7. Gauer R, Meyers BK. Heat-related illnesses. American family physician. 2019;99(8):482-9.

8. Wijerathna-Yapa A, Pathirana R. Sustainable agro-food systems for addressing climate change and food security. Agriculture. 2022;12(10):1554.

9. Gamarro H, Ortiz L, González JE. Adapting to extreme heat: social, atmospheric, and infrastructure impacts of air-conditioning in megacities—The case of New York City. Journal of Engineering for Sustainable Buildings and Cities. 2020;1(3):031005.

10. Zhang Z, Kircher KJ, Cai Y, Brearley JG, Birge DP, Norford LK. Mitigating peak load and heat stress under heatwaves by optimizing adjustments of fan speed and thermostat setpoint. Journal of Building Performance Simulation. 2023;16(4):493-506.

11. Bandh SA, Shafi S, Peerzada M, Rehman T, Bashir S, Wani SA, et al. Multidimensional analysis of global climate change: a review. Environmental Science and Pollution Research. 2021;28(20):24872-88.

12. Wemegah CS, Yamba EI, Aryee JN, Sam F, Amekudzi LK. Assessment of urban heat island warming in the greater accra region. Scientific African. 2020;8:e00426.

13. Ceccherini G, Russo S, Ameztoy I, Marchese AF, Carmona-Moreno C. Heat waves in Africa 1981–2015, observations and reanalysis. Natural Hazards and Earth System Sciences. 2017;17(1):115-25.

14. Mora C, Dousset B, Caldwell IR, Powell FE, Geronimo RC, Bielecki CR, et al. Global risk of deadly heat. Nature climate change. 2017;7(7):501-6.

15. Crunch C. 58—Disaster Year in Review (2019). CRED: Brussels, Belgium. 2020.

16. Loboda T, Krankina O, Savin I, Kurbanov E, Hall J. Land management and the impact of the 2010 extreme drought event on the agricultural and ecological

systems of European Russia. Land-Cover and Land-Use Changes in Eastern Europe after the Collapse of the Soviet Union in 1991. 2017:173-92.

17. Mbokodo I, Bopape MJ, Chikoore H, Engelbrecht F, Nethengwe N. Heatwaves in the future warmer climate of South Africa. Atmosphere. 2020;11(7):712.

18. Birch C, Jackson L, Finney D, Marsham J, Stratton R, Tucker S, et al. Future changes in African heatwaves and their drivers at the convective scale. Journal of Climate. 2022;35(18):5981-6006.

19. Barnes C, Otto F, Clarke B, Pinto I, Guigma K, Savadogo I, et al. Extreme Sahel Heatwave that Hit Highly Vulnerable Population at the End of Ramadan Would Not Have Occurred without Climate Change. Imperial College of London. Report of the World Weather Attribution Project. 2024.

20. Yamba EI, Aryee JN, Quansah E, Davies P, Wemegah CS, Osei MA, et al. Revisiting the agro-climatic zones of Ghana: A re-classification in conformity with climate change and variability. PLOS Climate. 2023;2(1):e0000023.

21. Wemegah CS, Yamba EI, Quansah E, Nyantakyi EK, Amekudzi LK. Evidence of heatwaves: characteristics and trends in selected ghanaian cities. International Journal of Climatology. 2025;45(10):e8889.

22. Adjei MJ, Yamba EI, Tuholske C, Wemegah CS, Amekudzi LK. Assessing heat-related health risk in Ghana using bioclimatic indices. Scientific African. 2025:e02926.

23. Klutse NAB, Owusu K, Boafo YA. Projected temperature increases over northern Ghana. SN Applied Sciences. 2020;2:1-14.

24. Brunner L, Voigt A. Revealing a systematic bias in percentile-based temperature extremes. European Geosciences Union General Assembly 2024 (EGU24). 2024:1722.

25. Nairn JR, Fawcett RJ. The excess heat factor: a metric for heatwave intensity and its use in classifying heatwave severity. International journal of environmental research and public health. 2015;12(1):227-53.

26. Nairn J, Ostendorf B, Bi P. Performance of Excess Heat Factor Severity as a Global Heatwave Health Impact Index. International Journal of Environmental Research and Public Health. 2018;15(11):2494. doi:10.3390/ijerph15112494.

27. Basarin B, Lukić T, Matzarakis A. Review of biometeorology of heatwaves and warm extremes in Europe. Atmosphere. 2020;11(12):1276.

28. Malcheva K, Bocheva L, Chervenkov H. Spatio-Temporal Variation of Extreme Heat Events in Southeastern Europe. Atmosphere. 2022;13(8):1186.

29. Tao J, Xu Z, Ho HC, Zheng H, Xing X, Hu J, et al. Quantifying localized heatwave impact on mortality: a multi-country modeling study in the Asia–Pacific region. The Lancet Regional Health–Western Pacific. 2025;61.

30. Scalley BD, Spicer T, Jian L, Xiao J, Nairn J, Robertson A, et al. Responding to heatwave intensity: excess heat factor is a superior predictor of health service utilisation and a trigger for heatwave plans. Australian and New Zealand journal of public health. 2015;39(6):582-7.

31. Tolika K. Assessing heat waves over Greece using the excess heat factor (EHF). Climate. 2019;7(1):9.

32. Ansah S, Ahiataku M, Yorke C, Otu-Larbi F, Yahaya B, Lamptey P, et al. Meteorological analysis of floods in Ghana. Advances in Meteorology. 2020;2020(1):4230627.

33. Aryee J, Amekudzi L, Quansah E, Klutse N, Atiah W, Yorke C. Development of high spatial resolution rainfall data for Ghana. International Journal of Climatology. 2018;38(3):1201-15.

34. Amekudzi LK, Yamba EI, Preko K, Asare EO, Aryee J, Baidu M, et al. Variabilities in rainfall onset, cessation and length of rainy season for the various agro-ecological zones of Ghana. Climate. 2015;3(2):416-34.

35. Effects of anthropogenic fires on some soil properties and the implications of fire frequency for the Guinea savanna ecological zone, Ghana. Scientific African. 2019;6:e00201. doi:https://doi.org/10.1016/j.sciaf.2019.e00201.

36. Ampofo S, Annor T, Aryee JN, Atiah WA, Amekudzi LK. Long-term spatio-temporal variability and change in rainfall over Ghana (1960–2015). Scientific African. 2023;19:e01588.

37. Hersbach H, Bell B, Berrisford P, Hirahara S, Horányi A, Muñoz-Sabater J, et al. The ERA5 global reanalysis. Quarterly Journal of the Royal Meteorological Society. 2020;146(730):1999-2049.

38. Gleixner S, Demissie T, Diro GT. Did ERA5 improve temperature and precipitation reanalysis over East Africa? Atmosphere. 2020;11(9):996.

39. Parsons D, Stern D, Ndanguza D, Sylla MB. Evaluation of satellite-based air temperature estimates at eight diverse sites in Africa. Climate. 2022;10(7):98.

40. Katsekpor JT, Greve K, Yamba EI, Amoah EG. Comparative analysis of satellite and reanalysis data with ground-based observations in Northern Ghana. Meteorological Applications. 2024;31(4):e2226.

41. Chanda K, Maity R. Meteorological drought quantification with standardized precipitation anomaly index for the regions with strongly seasonal and periodic precipitation. Journal of Hydrologic Engineering. 2015;20(12):06015007.

42. Hamdi I, AbdAlmapoed EK, AbdElaal SR. Assessment of Urban Heat Island Effects in Industrial Areas of Egypt using Robust Statistical Methods. Remote Sensing Applications: Society and Environment. 2025:101777.

43. Langlois N, Herbst J, Mason K, Nairn J, Byard RW. Using the Excess Heat Factor (EHF) to Predict the Risk of Heat Related Deaths. Journal of Forensic and Legal Medicine. 2013;20(5):408-11. doi:10.1016/j.jflm.2013.02.004.

44. Hatvani-Kovacs G, Belusko M, Pockett J, Boland J. Can the Excess Heat Factor Indicate Heatwave-Related Morbidity? A Case Study in Adelaide, South Australia. EcoHealth. 2016;13(1):100-10. doi:10.1007/s10393-015-1085-5.

45. Raei E, Nikoo MR, AghaKouchak A, Mazdiyasni O, Sadegh M. GHWR, a multi-method global heatwave and warm-spell record and toolbox. Scientific data. 2018;5(1):180206.

46. Davison AC, Smith RL. Models for Exceedances over High Thresholds. Journal of the Royal Statistical Society: Series B (Methodological). 1990;52(3):393-442. doi:10.1111/j.2517-6161.1990.tb01796.x.

47. Coles S, Bawa J, Trenner L, Dorazio P. An introduction to statistical modeling of extreme values. vol. 208. Springer; 2001.

48. Scarrott C, MacDonald A. A Review of Extreme Value Threshold Estimation and Uncertainty Quantification. REVSTAT – Statistical Journal. 2012;10(1):33-60. doi:10.57805/revstat.v10i1.110.

49. Bader B, Yan J, Zhang X. Automated Threshold Selection for Extreme Value Analysis via Ordered Goodness-of-Fit Tests with Adjustment for False Discovery Rate. The Annals of Applied Statistics. 2018;12(1):310-29. doi:10.1214/17-AOAS1092.

50. Kyselý J. A Cautionary Note on the Use of Nonparametric Bootstrap for Estimating Uncertainties in Extreme-Value Models. Journal of Applied Meteorology and Climatology. 2008;47(12):3236-51. doi:10.1175/2008JAMC1763.1.

51. Huang WK, Stein ML, McInerney DJ, Sun S, Moyer EJ. Estimating changes in temperature extremes from millennial-scale climate simulations using generalized extreme value (GEV) distributions. Advances in Statistical Climatology, Meteorology and Oceanography. 2016;2(1):79-103.

52. Hasan H, Salam N, Kassim S. Modeling annual extreme temperature using generalized extreme value distribution: A case study in Malaysia. In: AIP Conference Proceedings. vol. 1522. American Institute of Physics; 2013. p. 1195-203.

53. Padoan SA. Extreme value analysis. Wiley StatsRef: Statistics Reference Online. 2014.

54. Masson-Delmotte V, Zhai P, Pörtner HO, Roberts D, Skea J, Shukla PR, et al. Global warming of 1.5 C. An IPCC Special Report on the impacts of global warming. 2019;1:93-174.

55. Doan QV, Chen F, Asano Y, Gu Y, Nishi A, Kusaka H, et al. Causes for asymmetric warming of sub-diurnal temperature responding to global warming. Geophysical Research Letters. 2022;49(20):e2022GL100029.

56. Carter AW, Fleming JM. Hotter Nights, Hidden Consequences: An Overlooked Dimension of Climate Change. Integrative and Comparative Biology. 2025;65(4):832-49.

57. He C, Kim H, Hashizume M, Lee W, Honda Y, Kim SE, et al. The effects of night-time warming on mortality burden under future climate change scenarios: a modelling study. The Lancet Planetary Health. 2022;6(8):e648-57.

58. Braimah M, Asante VA, Ahiataku MA, Ansah SO, Otu-Larbi F, Yahaya B, et al. Variability of the minor season rainfall over southern Ghana (1981–2018). Advances in Meteorology. 2022;2022(1):1861130.

59. Cook KH, Vizy EK. Impact of climate change on mid-twenty-first century growing seasons in Africa. Climate Dynamics. 2012;39:2937-55.

60. Ampim PA, Ogbe M, Obeng E, Akley EK, MacCarthy DS. Land cover changes in Ghana over the past 24 years. Sustainability. 2021;13(9):4951.

61. Adeyeri OE. A synthesis of compound drought in Africa: Mechanisms, hotspots, impacts, and future projections. Water. 2026;18(9):1040.

62. Nooni IK, Ogou FK, Saidou Chaibou AA, Fianko SK, Atta-Darkwa T, Prempeh NA. Relative humidity and air temperature characteristics and their drivers in africa tropics. Atmosphere. 2025;16(7):828.

63. Isaac T, Ranjith S, Latha P, Shanmugam R, Venugopal V. Physiological strain in outdoor workers: The hidden danger of high humidity. Environmental Research. 2025;276:121495.

64. Vanos J, Guzman-Echavarria G, Baldwin JW, Bongers C, Ebi KL, Jay O. A physiological approach for assessing human survivability and liveability to heat in a changing climate. Nature communications. 2023;14(1):7653.

65. Wei J, Han W, Wang W, Zhang L, Rajagopalan B. Intensification of heatwaves in China in recent decades: Roles of climate modes. npj Climate and Atmospheric Science. 2023;6(1):98.

66. Joly M, Voldoire A. Influence of ENSO on the West African monsoon: temporal aspects and atmospheric processes. Journal of Climate. 2009;22(12):3193-210.

67. Russo S, Marchese AF, Sillmann J, Immé G. When will unusual heat waves become normal in a warming Africa? Environmental Research Letters. 2016;11(5):054016.

68. Iyakaremye V, Zeng G, Ullah I, Gahigi A, Mumo R, Ayugi B. Recent observed changes in extreme high-temperature events and associated meteorological conditions over Africa. Int J Climatol. 2022;42(9):4522-37.

69. Engdaw MM, Ballinger AP, Hegerl GC, Steiner AK. Changes in temperature and heat waves over Africa using observational and reanalysis data sets. International Journal of Climatology. 2022;42(2):1165-80.

70. Oduro C, Lim Kam Sian KTC, Hagan DFT, Babaousmail H, Ayugi BO, Wu Y, et al. The influence of land surface temperature on Ghana's climate variability and implications for sustainable development. Scientific Reports. 2025;15(1):2595.

71. Ngoungue Langue CG, Lavaysse C, Vrac M, Flamant C. Heat wave monitoring over West African cities: uncertainties, characterization and recent trends. Natural Hazards and Earth System Sciences. 2023;23(4):1313-33.

72. Pinto I, Odoulami R, Lawal K, Olaniyan E, Ibrahim W, Guigma K, et al. Dangerous humid heat in southern West Africa about 4 C hotter due to climate change. World Weather Attribution https://www worldweatherattribution org/dangerous-humid-heat-in-southern-west-africa-about-4c-hotter-due-to-climate-change. 2024.

73. Guigma KH, MacLeod D, Todd M, Wang Y. Prediction skill of Sahelian heatwaves out to subseasonal lead times and importance of atmospheric tropical modes of variability. Climate Dynamics. 2021;57(1):537-56.

74. Issa MA, Chebana F, Masselot P, Campagna C, Lavigne É, Gosselin P, et al. A heat-health watch and warning system with extended season and evolving thresholds. BMC public health. 2021;21(1):1479.

75. Ankrah J, Monteiro A, Madureira H. Extreme temperature and rainfall events and future climate change projections in the coastal savannah agroecological zone of Ghana. Atmosphere. 2023;14(2):386.

Fig 1: The map of Ghana showing the different climate zones and the respective stations from which data are used. Adapted from Yamba et. al. [20]

Fig 2: Trends in standardized anomalies of annual Tmax, Tmin, and Tmean

Fig 3: Heatwave episodes in the Sudan Savannah zone (Navrongo, Zuarungu). Bar position marks the day-of-year of onset, bar height the episode duration, and colour the mean EHF intensity.

Fig 4: Heatwave episodes in the Guinea Savannah zone (Wa, Bole, Tamale, Yendi, Kete Krachi). Bar position marks the day-of-year of onset, bar height the episode duration, and colour the mean EHF intensity.

Fig 5: Heatwave episodes in the Transition zone (Sunyani, Wenchi). Bar position marks the day-of-year of onset, bar height the episode duration, and colour the mean EHF intensity.

Fig 6: Heatwave episodes in the Forest zone (Ho, Kumasi, Akim Oda, Sefwi Bekwai). Bar position marks the day-of-year of onset, bar height the episode duration, and colour the mean EHF intensity.

Fig 7: Heatwave episodes in the Coastal zone (Accra, Akatsi, Tema). Bar position marks the day-of-year of onset, bar height the episode duration, and colour the mean EHF intensity.

Fig 8: Total heatwave days and 5-year rolling mean trends over the climatic zones.

Fig 9: Return period of heatwave intensity and duration across the five climatic zones of Ghana.

Supporting information

Fig SM1 – SM5 show, for each station, the daily maximum temperature records classified by the quality-control flags: valid values (within the dashed 15–45 °C thresholds), and the categories flagged and assigned the placeholder −99 (non-numeric entries, outliers outside the plausible range, missing dates, Tmin > Tmax, and an implausible Tmax − Tmin spread), prior to gap-filling with ERA5. Flagged categories are plotted at fixed negative positions. The figures indicate both the coverage of each station and the periods most affected by missing or flagged data.

Fig SM1: Quality-control flag overview for daily maximum temperature at the Sudan Savannah stations (Navrongo, Zuarungu), 1960–2022.

Fig SM2: Quality-control flag overview for daily maximum temperature at the Guinea Savannah stations (Wa, Bole, Tamale, Yendi, Kete Krachi), 1960–2022.

Fig SM3: Quality-control flag overview for daily maximum temperature at the Transition stations (Sunyani, Wenchi), 1960–2022.

Fig SM4: Quality-control flag overview for daily maximum temperature at the Forest stations (Ho, Kumasi, Akim Oda, Sefwi Bekwai), 1960–2022.

Fig SM5: Quality-control flag overview for daily maximum temperature at the Coastal stations (Accra, Akatsi, Tema), 1960–2022.

Climate Zones of Ghana

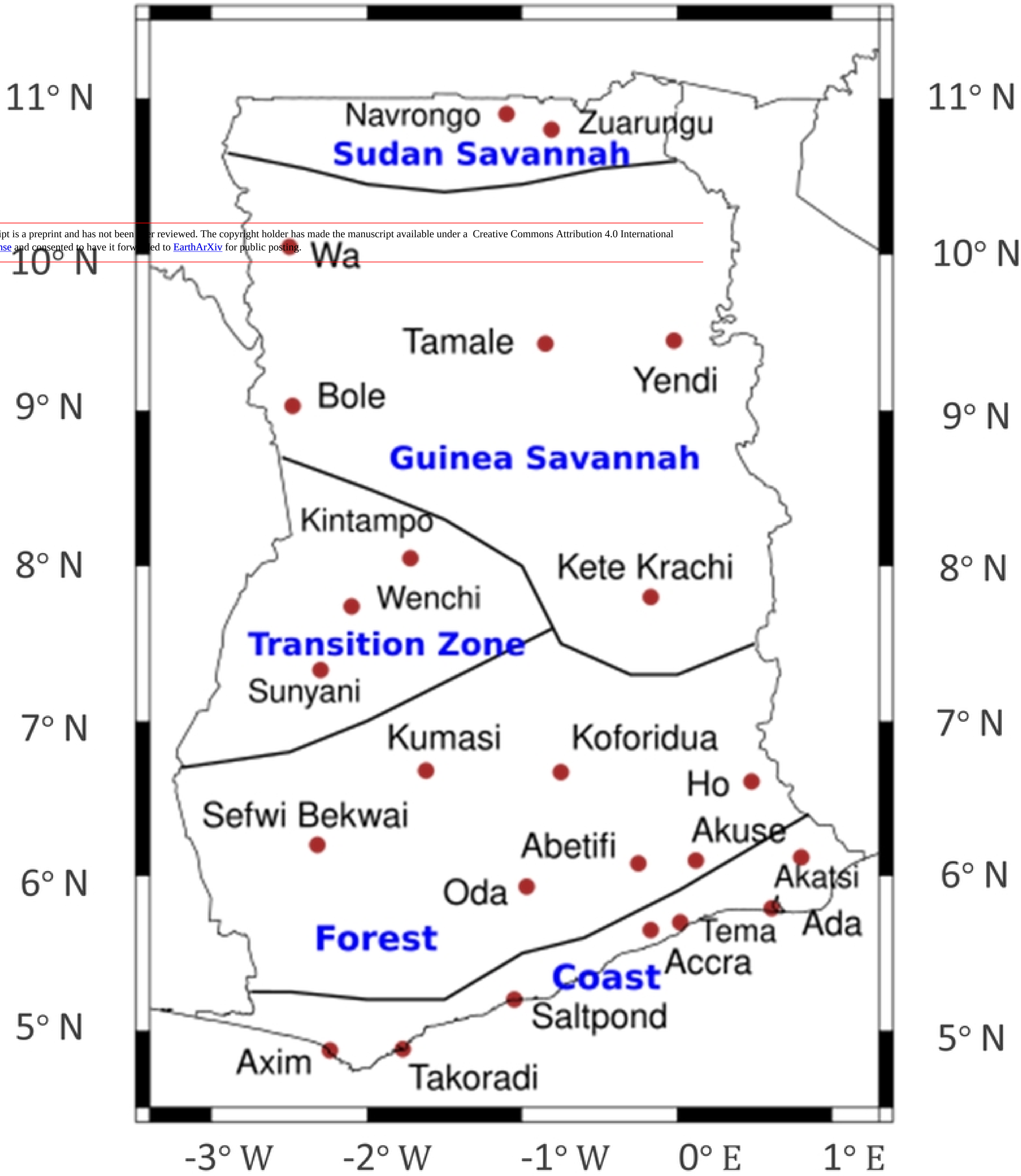

Figure

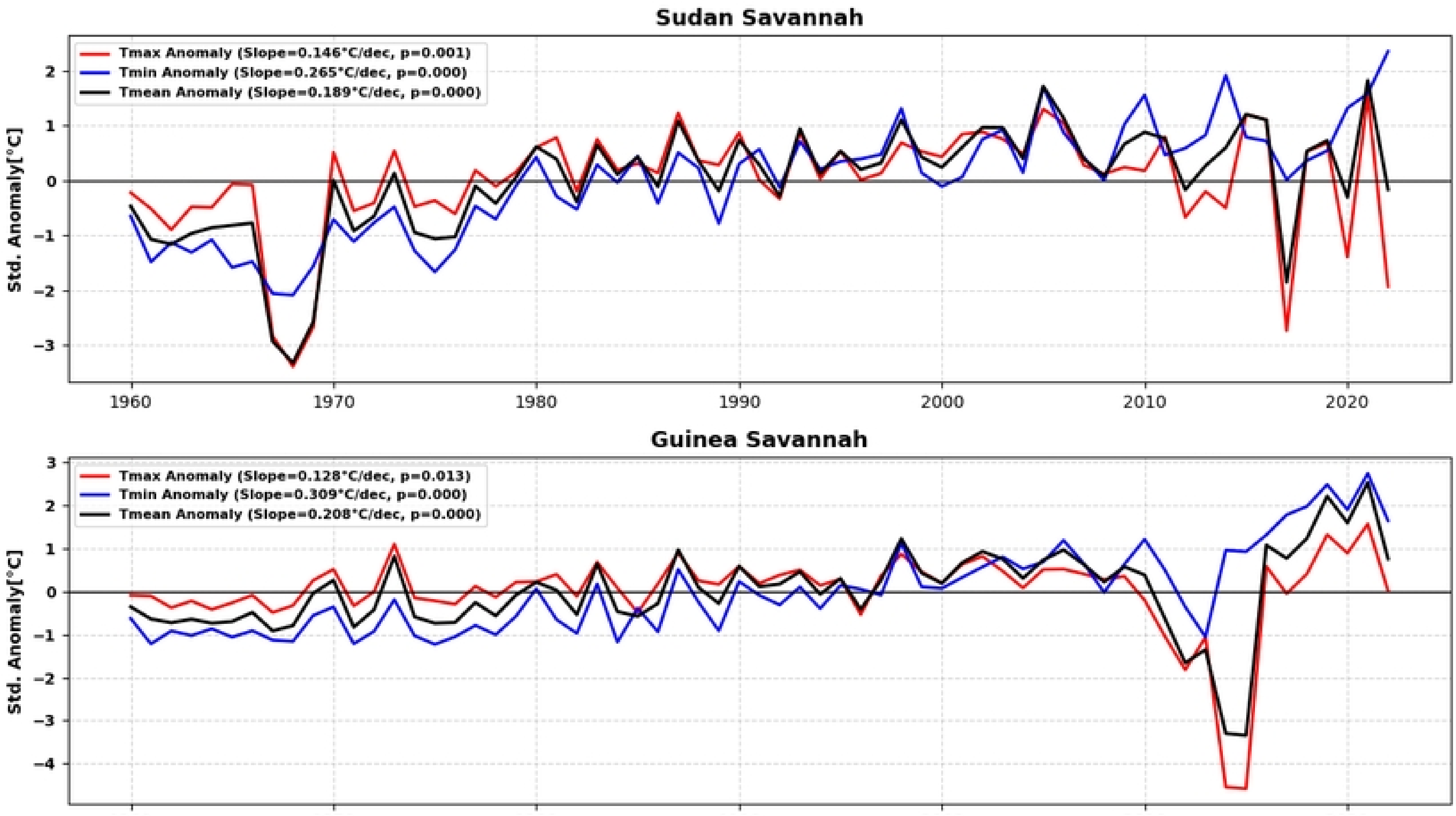
Sudan Savannah
Tmax Anomaly (Slope=0.146°C/dec, p=0.001)
Tmin Anomaly (Slope=0.265°C/dec, p=0.000)
Tmean Anomaly (Slope=0.189°C/dec, p=0.000)
Std. Anomaly[°C]
Guinea Savannah
Tmax Anomaly (Slope=0.128°C/dec, p=0.013)
Tmin Anomaly (Slope=0.309°C/dec, p=0.000)
Tmean Anomaly (Slope=0.208°C/dec, p=0.000)
Std. Anomaly[°C]

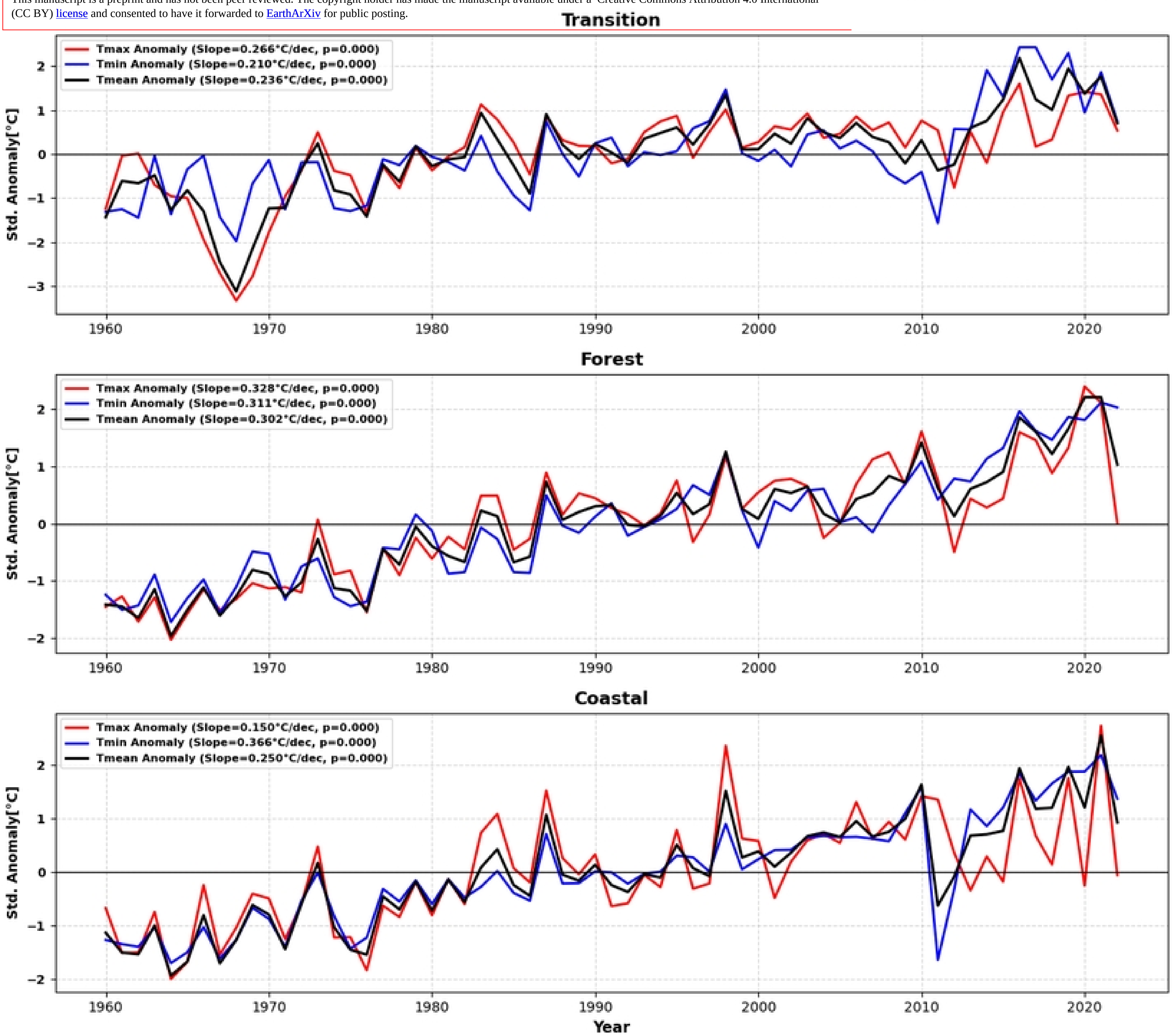
Transition
Tmax Anomaly (Slope=0.266°C/dec, p=0.000)
Tmin Anomaly (Slope=0.210°C/dec, p=0.000)
Tmean Anomaly (Slope=0.236°C/dec, p=0.000)
Std. Anomaly[°C]
Forest
Tmax Anomaly (Slope=0.328°C/dec, p=0.000)
Tmin Anomaly (Slope=0.311°C/dec, p=0.000)
Tmean Anomaly (Slope=0.302°C/dec, p=0.000)
Std. Anomaly[°C]
Coastal
Tmax Anomaly (Slope=0.150°C/dec, p=0.000)
Tmin Anomaly (Slope=0.366°C/dec, p=0.000)
Tmean Anomaly (Slope=0.250°C/dec, p=0.000)
Std. Anomaly[°C]
Year

Figure

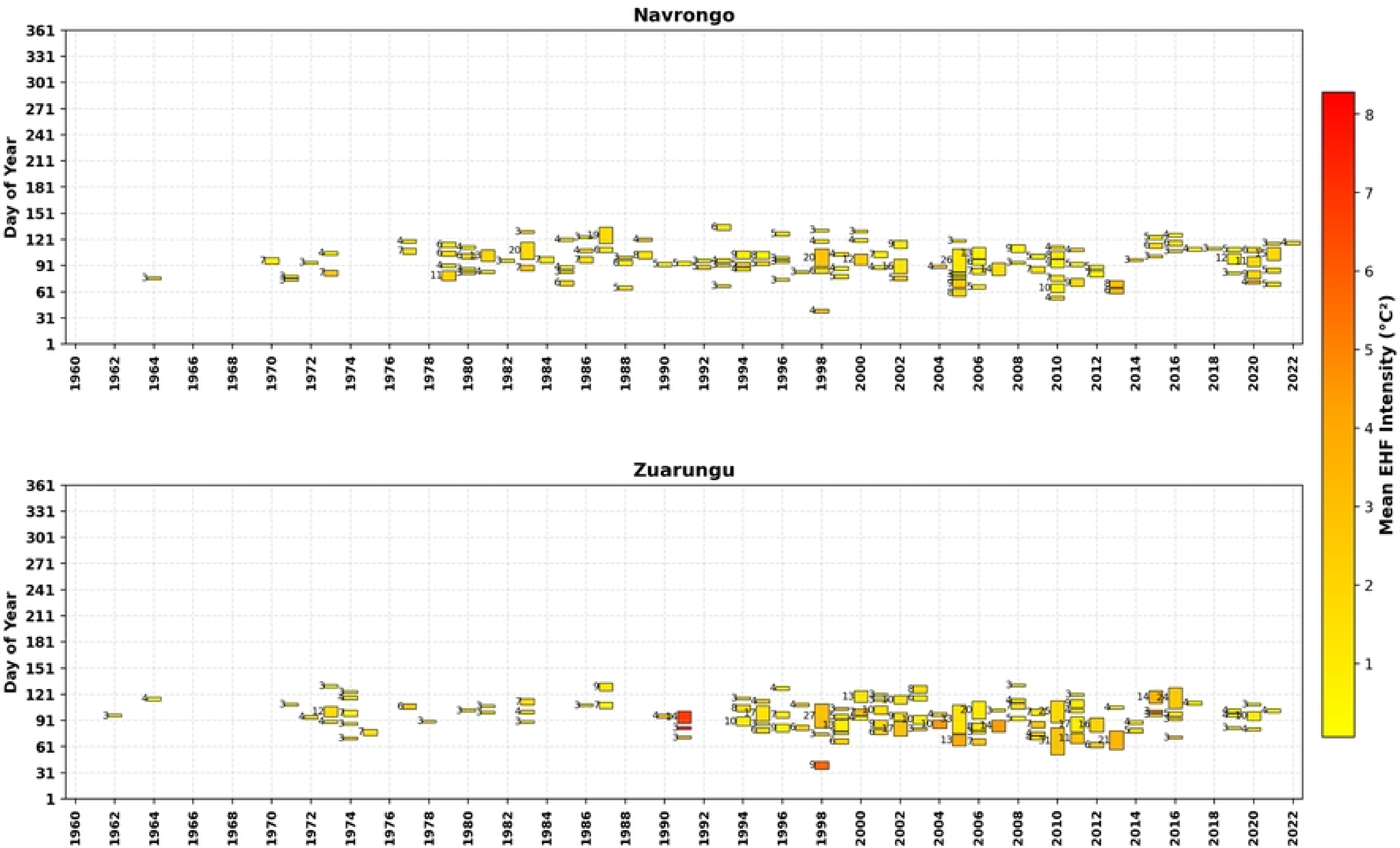

Figure

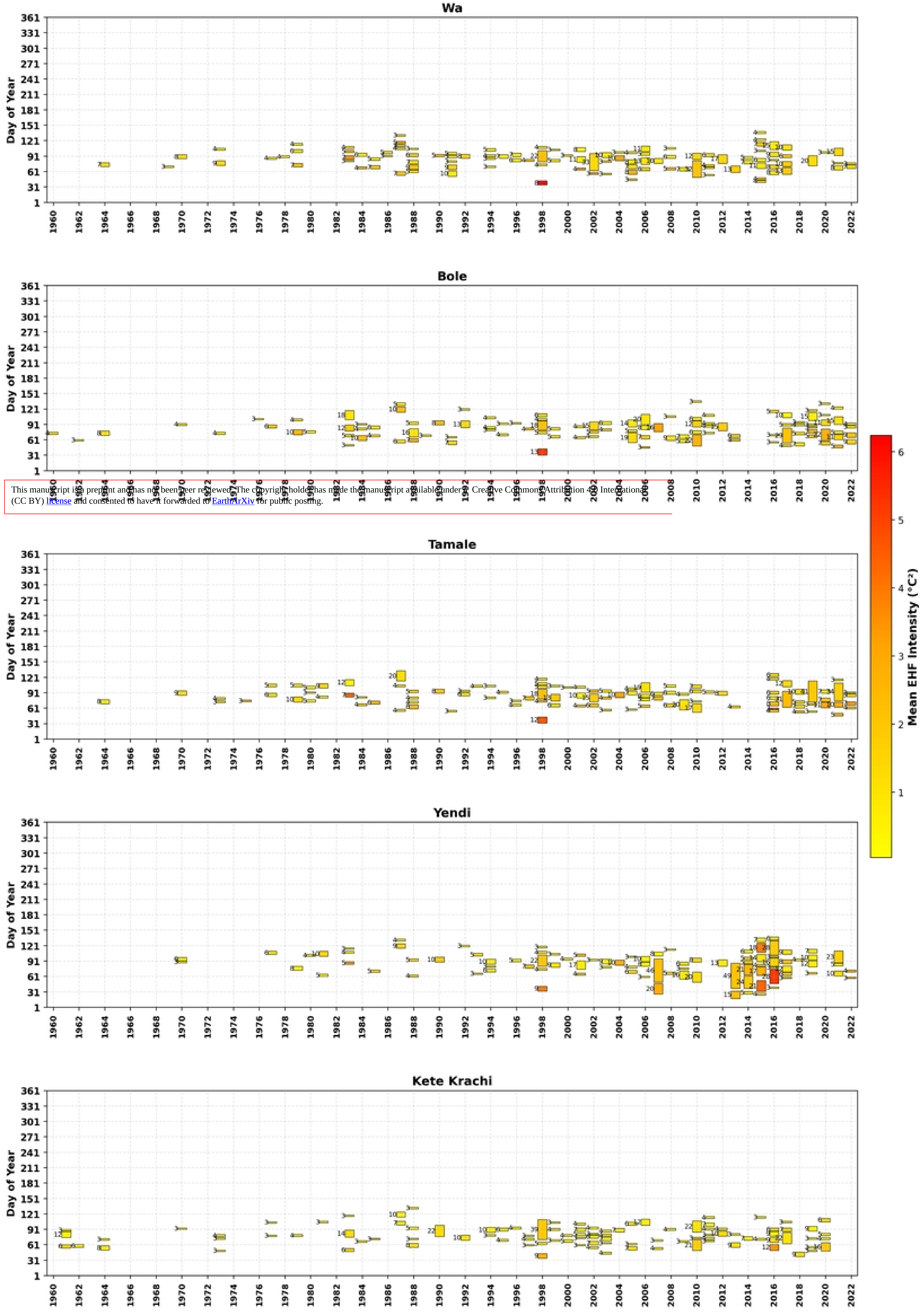
Wa
Bole
Tamale
Yendi
Kete Krachi
Day of Year
Mean EHF Intensity (°C²)

Figure

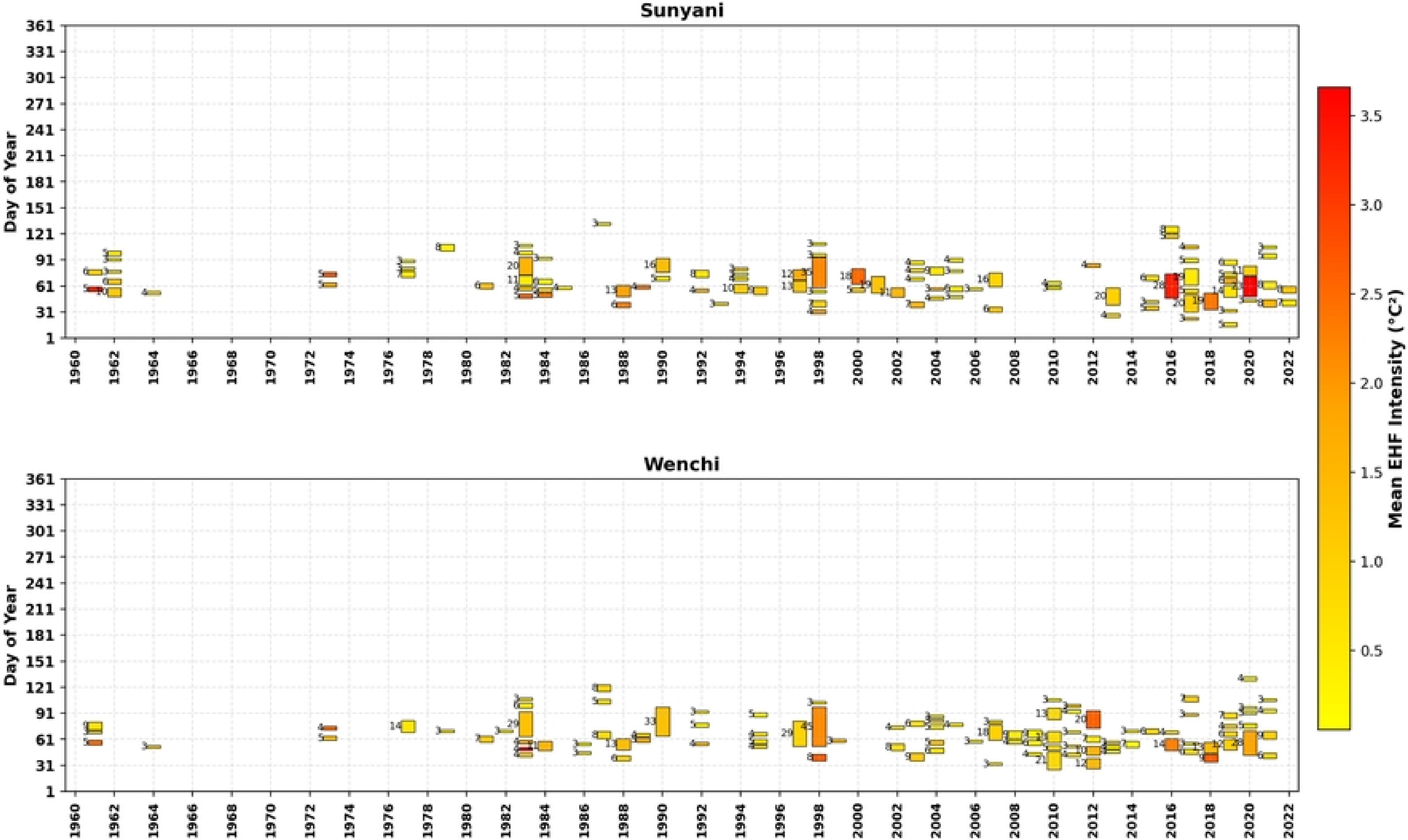

Figure

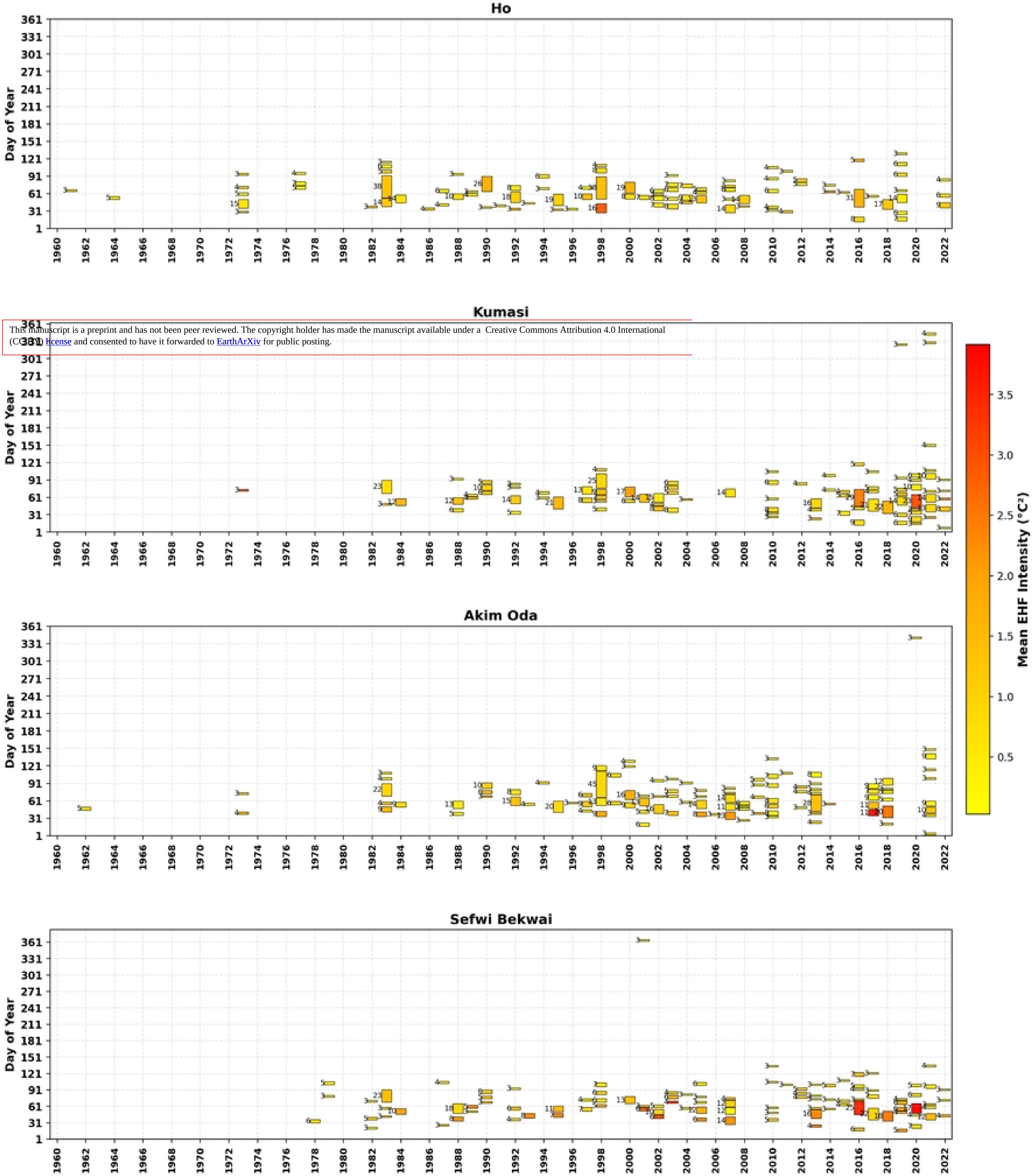
Ho
Kumasi
Akim Oda
Sefwi Bekwai
Day of Year
Mean EHF Intensity (°C²)

Figure

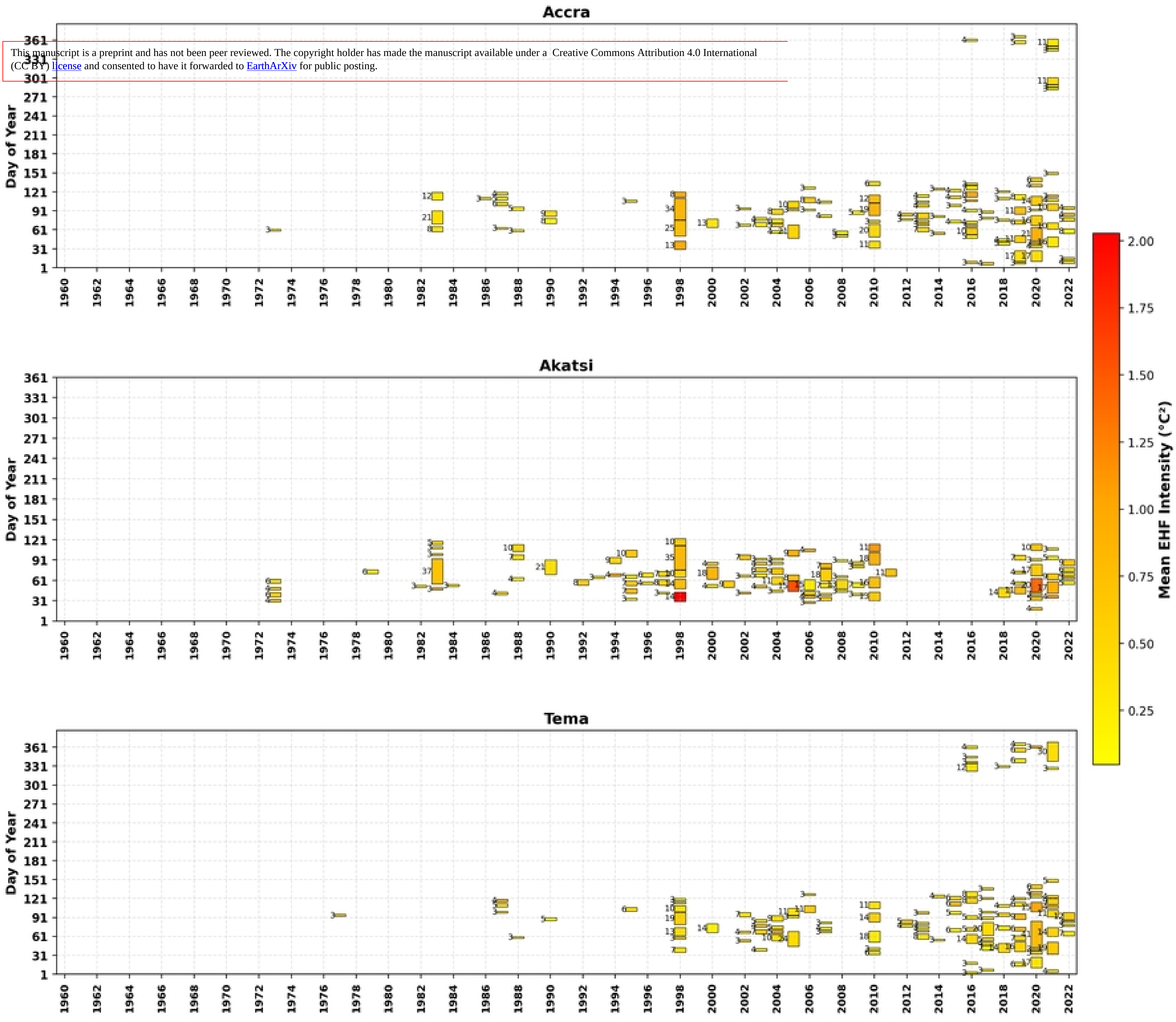

Figure

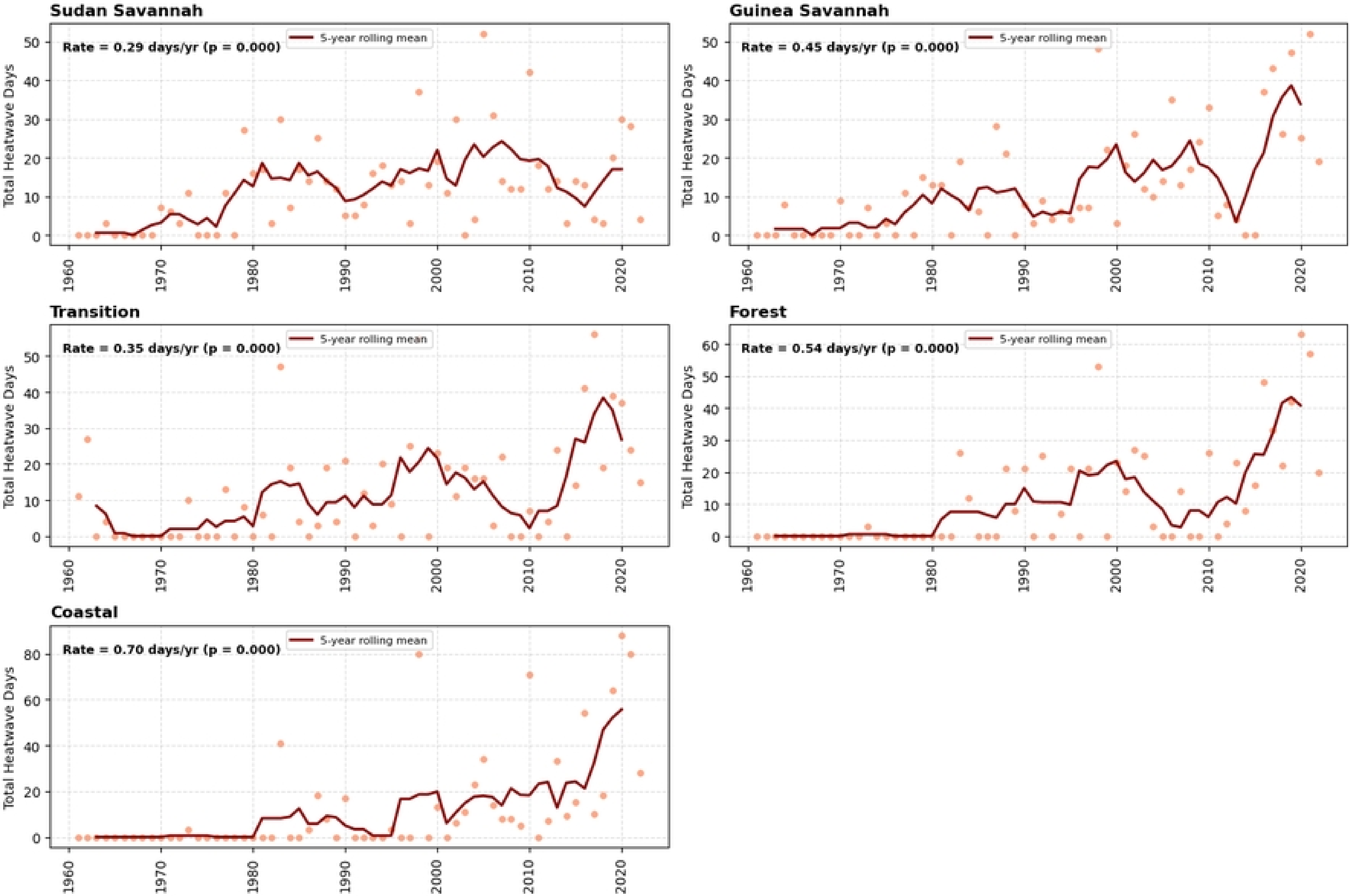
Sudan Savannah
Rate = 0.29 days/yr (p = 0.000)
5-year rolling mean
Guinea Savannah
Rate = 0.45 days/yr (p = 0.000)
5-year rolling mean
Transition
Rate = 0.35 days/yr (p = 0.000)
5-year rolling mean
Forest
Rate = 0.54 days/yr (p = 0.000)
5-year rolling mean
Coastal
Rate = 0.70 days/yr (p = 0.000)
5-year rolling mean
Total Heatwave Days
1960
1970
1980
1990
2000
2010
2020

Figure

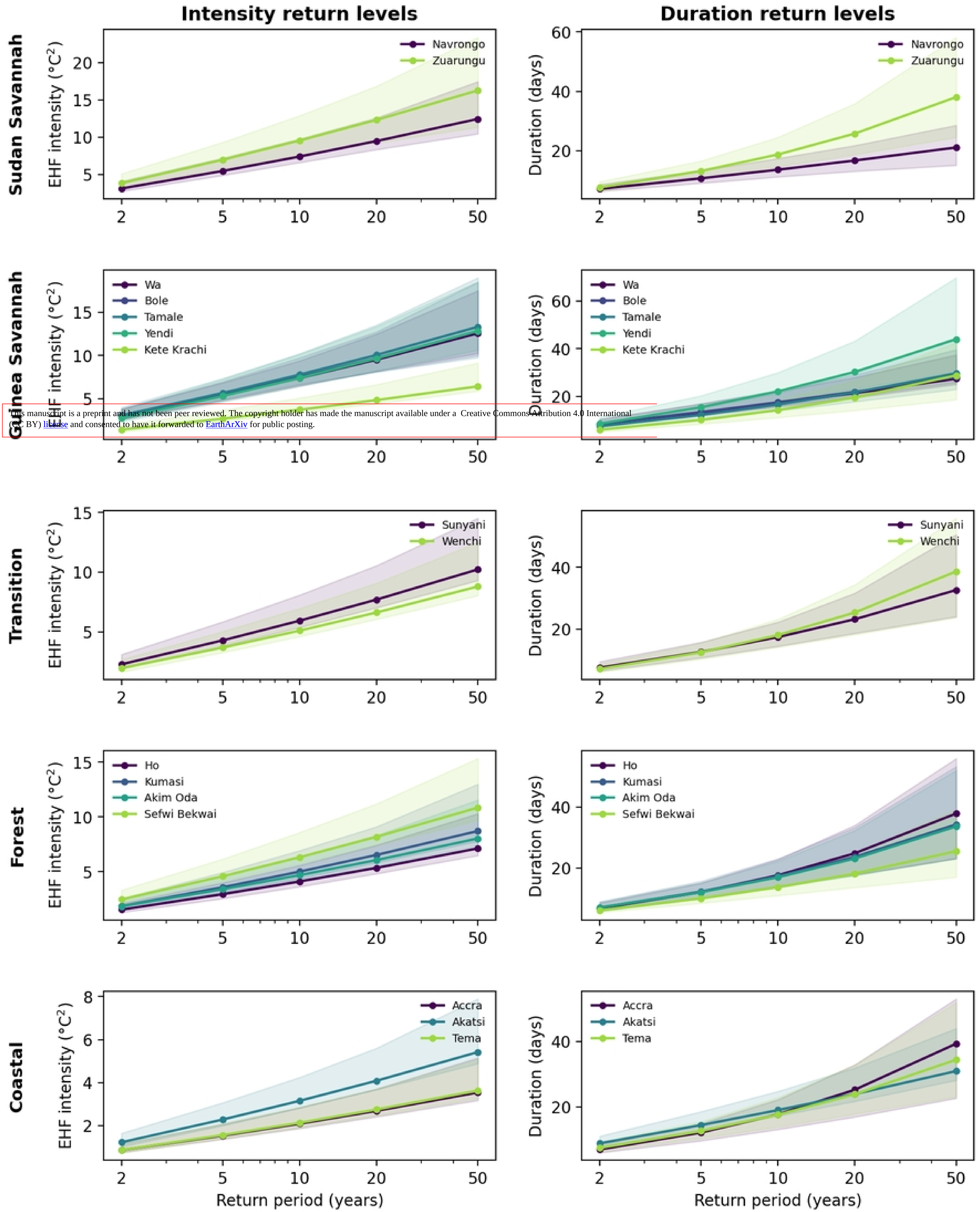

Intensity return levels
Duration return levels
Sudan Savannah
Guinea Savannah
Transition
Forest
Coastal
EHF intensity (°C²)
Duration (days)
Return period (years)
Navrongo
Zuarungu
Wa
Bole
Tamale
Yendi
Kete Krachi
Sunyani
Wenchi
Ho
Kumasi
Akim Oda
Sefwi Bekwai
Accra
Akatsi
Tema

Figure